

Doctoral Thesis

Topological Stability and Preconditioning of Higher-Order Laplacian Operators on Simplicial Complexes

PhD Program in Mathematics: XXXV cycle

Supervisor:

Author:

Anton Savostianov
anton.savostianov@gssi.it

Prof. Francesco Tudisco and
Prof. Nicola Guglielmi
francesco.tudisco@gssi.it &
nicola.guglielmi@gssi.it

October 2023

Abstract

 Insert here the abstract of the thesis proposal.

Contents

| | |
|--|-----------|
| Abstract | i |
| List of Figures | iv |
| List of Tables | vi |
| 1 Introduction | 1 |
| 2 Simplicial complex as Higher-order Topology Description | 2 |
| 2.1 From graph to higher-order models | 2 |
| 2.2 Simplicial Complexes | 2 |
| 2.3 Hodge's Theory | 4 |
| 2.4 Boundary and Laplacian Operators | 6 |
| 2.4.1 Boundary operators B_k | 6 |
| 2.4.2 Homology group and Hodge Laplacians L_k | 9 |
| 2.4.2.1 Homology group as Quontinent space | 9 |
| 2.4.2.2 Elements of the Hodge decomposition as harmonic/vorticity/potential flow | 10 |
| 2.4.2.3 Laplacian operators L_k | 12 |
| 2.4.2.4 Classical Laplacian and its kernel elements | 12 |
| 2.4.2.5 Kernel elements of L_k | 13 |
| Spreading and balancing as a mechanism of the non-local circulation | 13 |
| 2.5 Weigthed and Normalised Boundary Operators | 13 |
| 3 Topological Stability as MNP | 15 |
| 3.1 General idea of the topological stability | 15 |
| 3.1.1 Alternative with a persistent homology | 15 |
| 3.1.2 Transition to the spectral properties | 15 |
| 3.2 101 on Spectral Matrix Nearness Problems | 15 |
| 3.2.1 Functional and Gradient Flow | 16 |
| 3.2.2 Transition to the gradient flow | 16 |
| 3.2.3 Constraint gradient flow | 16 |
| 3.2.4 Sparsity pattern and rank-1 optimizers | 16 |
| 3.2.5 Idea of two level optimization | 16 |
| 3.3 Direct approach: failure and discontinuity problems | 16 |
| 3.3.1 Principal spectral inheritance | 16 |
| 3.3.2 Example with inherited disconnectedness | 18 |

| | | |
|----------|--|-----------|
| 3.3.3 | Example with faux edges (different weighting scheme) | 18 |
| 3.4 | Functional, derivative and alternating scheme | 18 |
| 3.4.1 | Target Functional | 18 |
| 3.4.2 | Free gradient calculation | 18 |
| 3.4.3 | The constrained gradient system and its stationary points | 20 |
| 3.4.4 | Constrained gradient | 21 |
| 3.4.5 | Alternating scheme | 21 |
| 3.4.6 | Implementation | 21 |
| 3.4.6.1 | Algorithms | 21 |
| 3.4.6.2 | Computation of the first non-zero eigenvalue | 21 |
| 3.4.6.3 | Preconditioning in the eigen-phase | 21 |
| 3.5 | Benchmarking | 21 |
| 3.5.1 | Illustrative Example | 21 |
| 3.5.2 | Triangulation Benchmark | 23 |
| 3.5.3 | Transportation Networks | 25 |
| 4 | Preconditioning | 28 |
| 4.1 | Preconditioning 101 | 28 |
| 4.1.1 | why do we care about the condition number? | 28 |
| 4.1.2 | Iterative methods | 28 |
| 4.1.3 | CG and convergence | 28 |
| 4.1.4 | Zoo of preconditioners | 28 |
| 4.2 | LSq problem for the whole Laplacian \rightarrow up-Laplacian | 29 |
| 4.3 | Preconditioning on the up-Laplacian | 29 |
| 4.3.1 | Sparsification (Spielman/Osting) | 29 |
| 4.3.2 | Cholesky preconditioning for classical graphs | 29 |
| 4.3.2.1 | Stochastic Cholesky preconditioning | 29 |
| 4.3.2.2 | Schur complements | 29 |
| 4.3.3 | Problem with Schur complements in the case of L_1 | 29 |
| 4.4 | Collapsible simplicial complexes | 29 |
| 4.4.1 | Classical collapsibility | 29 |
| 4.4.2 | Weak collapsibility | 32 |
| 4.4.3 | Computational cost of the greedy algorithm | 33 |
| 4.5 | HeCS preconditioning | 34 |
| 4.5.1 | Constructing Heavy Subcomplex out of 2-Core | 39 |
| 4.5.2 | Cholesky decomposition for weakly collapsible subcomplex | 41 |
| 4.5.3 | Problem: precondition by subcomplex | 41 |
| 4.5.4 | Optimal weights for subsampling | 41 |
| 4.5.5 | Theorem on conditionality of a subcomplex | 41 |
| 4.5.6 | The notion of the heavy collapsible subcomplex | 41 |
| 4.5.7 | Algorithm and complexity | 41 |
| 4.6 | Benchmarking: triangulation | 41 |
| 4.6.1 | Timings of algorithm and preconditioned application | 41 |
| 4.6.2 | Conditionality and iterations | 41 |
| 4.6.3 | Compare with shifted ichol | 41 |
| 5 | Conclusion and future prospects | 42 |

List of Figures

| | | |
|-----|--|----|
| 2.1 | Example of a simplicial complex on 8 nodes; nodes included in the complex are shown in orange, edges — in black, and triangles — in blue. | 3 |
| 2.2 | Illustration of a harmonic representative for an equivalence class | 5 |
| 2.3 | Example of chains on the simplicial complex | 7 |
| 2.4 | Sample action of the boundary operators | 8 |
| 2.5 | Left-hand side panel: example of simplicial complex \mathcal{K} on 7 nodes, and of the action of B_2 on the 2-simplex $[1, 2, 3]$; 2-simplices included in the complex are shown in red, arrows correspond to the orientation. Panels on the right: matrix forms B_1 and B_2 of boundary operators respectively. | 9 |
| 2.6 | Continuous and analogous discrete manifolds with one 1-dimensional hole ($\dim \bar{\mathcal{H}}_1 = 1$). Left pane: the continuous manifold; center pane: the discretization with mesh vertices; right pane: a simplicial complex built upon the mesh. Triangles in the simplicial complex \mathcal{K} are colored gray (right). | 10 |
| 3.1 | Illustration for the principal spectrum inheritance (Theorem 3.1) in case $k = 0$: spectra of \bar{L}_1 , L_1^\perp and \bar{L}_1^\perp are shown. Colors signify the splitting of the spectrum, $\lambda_i > 0 \in \sigma(\bar{L}_1)$; all yellow eigenvalues are inherited from $\sigma_+(\bar{L}_0)$; red eigenvalues belong to the non-inherited part. Dashed barrier μ signifies the penalization threshold (see the target functional in ??) preventing homological pollution (see ??). | 17 |
| 3.2 | Simplicial complex \mathcal{K} on 8 vertices for the illustrative run (on the left): all 2-simplices from \mathcal{V}_2 are shown in blue, the weight of each edge $w_1(e_i)$ is given on the figure. On the right: perturbed simplicial complex \mathcal{K} through the elimination of the edge $[5, 6]$ creating additional hole $[5, 6, 7, 8]$ | 22 |
| 3.3 | Illustrative run of the framework determining the topological stability: the top pane — the flow of the functional $F(\varepsilon, E(t))$; the second pane — the flow of $\sigma(\bar{L}_1)$, λ_+ is highlighted; third pane — the change of the perturbation norm $\ E(t)\ $; the bottom pane — the heatmap of the perturbation profile $E(t)$ | 22 |
| 3.4 | Benchmarking Results on the Synthetic Triangulation Dataset: varying sparsities $\nu = 0.35, 0.5$ and $N = 16, 22, 28, 34, 40$; each network is sampled 10 times. Shapes correspond to the number of eliminated edges in the final perturbation: 1 : \circ , 2 : \square , 3 : \diamond , 4 : \triangle . For each pair (ν, N) , the un-preconditioned and Cholesky-preconditioned execution times are shown. | 24 |
| 3.5 | Example of the Transportation Network for Bologna. Left pane: original zone graph where the width of edges corresponds to the weight, to-be-eliminated edge is colored in red. Right pane: eigenflows, original and created; color and width correspond to the magnitude of entries. | 26 |

| | | |
|-----|--|----|
| 4.1 | Example of a simplicial complex: free simplices and maximal faces. . . . | 29 |
| 4.2 | 2-Core, examples. | 31 |
| 4.3 | The probability of the 2-Core in richer-than-triangulation simplicial complexes: triangulation of random points modified to have $\left\lceil \nu \frac{ \mathcal{V}_0(\mathcal{K}) \cdot (\mathcal{V}_0(\mathcal{K}) - 1)}{2} \right\rceil$ edges on the left; random sensor networks with ε -percolation on the right. ν_Δ defines the initial sparsity of the triangulated network; $\varepsilon_{\min} = \mathbb{E} \min_{x,y \in [0,1]^2} \ x - y\ _2$ is the minimal possible percolation parameter. | 32 |
| 4.4 | Example of weakly collapsible but not collapsible simplicial complex . . | 33 |
| 4.5 | The scheme of the simplicial complex transformation: from the original \mathcal{K} to the heavy weakly collapsible subcomplex \mathcal{L} | 40 |

List of Tables

| | | |
|-----|--|----|
| 3.1 | Topological instability of the transportation networks: filtered zone networks with the corresponding perturbation norm ε and its percentile among $w_1(\cdot)$ profile. For each simplicial complex the number of nodes, edges and triangles in $\mathcal{V}_2(\mathcal{K})$ are provided alongside the initial number of holes β_1 . The results of the algorithm consist of the perturbation norm, ε , computation time, and approximate percentile p . | 26 |
|-----|--|----|

Chapter 1

Introduction

Chapter 2

Simplicial complex as Higher-order Topology Description

2.1 From graph to higher-order models

 graph definition

 graph examples in real life (2 or 3)

 motivation for the transition to the higher order models

 Hypergraphs: definitions and examples

 Motifs: definitions and examples

 somehow relate to the tensor models and tractability simplicial complexes

2.2 Simplicial Complexes

Let $V = \{v_1, v_2, \dots, v_n\}$ be a set of nodes; as discussed above, such set may refer to various interacting entities and agents in the system, e.g. neurons, genes, traffic stops, online actors, publication authors, etc. Then:

Definition 2.1 (Simplicial Complex). The collection of subsets \mathcal{K} of the nodal set V is a (abstract) SC¹ if for each subset $\sigma \in \mathcal{K}$, referred as a simplex, all its subsets $\sigma', \sigma' \subseteq \sigma$, referred as faces, enter \mathcal{K} as well, $\sigma' \in \mathcal{K}$.

¹addition of the word “abstract” to the term is more common in the topological setting

We denote simplex σ on the set of vertices $\{u_1, u_2, \dots, u_{k+1}\} \in V$ as $\sigma = [u_1, u_2, \dots, u_{k+1}]$. Then, a simplex $\sigma \in \mathcal{K}$ on $k+1$ vertices is said to be of the order k , $\text{ord}(\sigma) = k$; alternatively, we refer to it as a k -order simplex or k -simplex. Let $\mathcal{V}_k(\mathcal{K})$ be a set of all k -order simplices in \mathcal{K} and m_k is the cardinality of $\mathcal{V}_k(\mathcal{K})$, $m_k = |\mathcal{V}_k(\mathcal{K})|$; then $\mathcal{V}_0(\mathcal{K})$ is the set of nodes in the simplicial complex \mathcal{K} , $\mathcal{V}_1(\mathcal{K})$ — the set of edges, $\mathcal{V}_2(\mathcal{K})$ — the set of triangles, or 3-cliques, and so on, with $\mathcal{K} = \{\mathcal{V}_0(\mathcal{K}), \mathcal{V}_1(\mathcal{K}), \mathcal{V}_2(\mathcal{K}), \dots\}$. Note that due to the inclusion rule in Definition 2.1, the number of non-empty $\mathcal{V}_k(\mathcal{K})$ is finite and, moreover, uninterrupted in a sense of the order: if $\mathcal{V}_k(\mathcal{K}) = \emptyset$, then $\mathcal{V}_{k+1}(\mathcal{K})$ is also necessarily empty.

Definition 2.2 (k -skeleton). For a given simplicial complex \mathcal{K} , a k -skeleton is defined as a simplicial complex $\mathcal{K}^{(k)}$ containing all simplices of \mathcal{K} of order at most k ,

$$\mathcal{K}^{(k)} = \bigcup_{i=0}^k \mathcal{V}_i(\mathcal{K}) \quad (2.1)$$

For instance, 2-skeleton of \mathcal{K} consists of all nodes, edges and triangles of \mathcal{K} .

It is easy to note that k -skeleton remains a simplicial complex: if $\sigma \in \mathcal{K}^{(k)}$, then all simplices τ from the original complex \mathcal{K} , $\text{ord}(\tau) \leq \text{ord}(\sigma)$, belong to $\mathcal{K}^{(k)}$ by definition; then, by inclusion principle, all faces σ' of σ belong to \mathcal{K} and $\text{ord}(\sigma') < \text{ord}(\sigma) \leq k$, so all faces of σ are necessarily included in the k -skeleton.

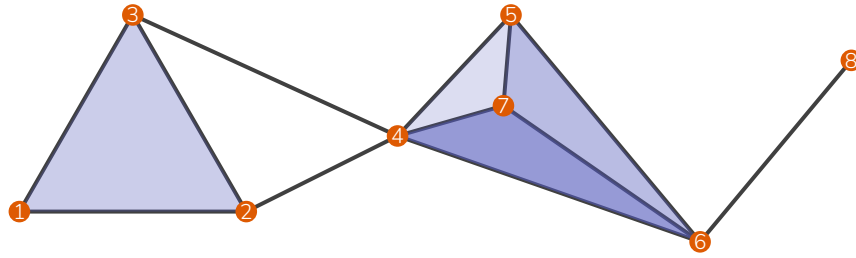


Figure 2.1: Example of a simplicial complex on 8 nodes; nodes included in the complex are shown in orange, edges — in black, and triangles — in blue.

Example 2.1 (Simplicial Complex). Here we provide the following example of the simplicial complex \mathcal{K} , Figure 2.1: we denote 0-order simplices (vertices) by orange color, 1-order simplices (edges) by black and 2-order simplices (triangles) by blue, where:

$$\begin{aligned} \mathcal{V}_0(\mathcal{K}) &= \{[1], [2], [3], [4], [5], [6], [7], [8]\} \\ \mathcal{V}_1(\mathcal{K}) &= \{[1, 2], [1, 3], [2, 3], [2, 4], [3, 4], [4, 5], [4, 6], [4, 7], [5, 6], [5, 7], [6, 7], [6, 8]\} \\ \mathcal{V}_2(\mathcal{K}) &= \{[1, 2, 3], [4, 5, 7], [4, 6, 7], [5, 6, 7]\} \end{aligned} \quad (2.2)$$

Note that $\mathcal{V}_3(\mathcal{K}) = \emptyset$, so the highest order of simplices in \mathcal{K} is 2. Additionally, edge $[4, 5]$, $[4, 6]$ and $[5, 6]$ are included in \mathcal{K} , but the triangle $[4, 5, 6]$ is not; this does not violate

the inclusion rule. Instead, every edge and every vertices of every triangle in $\mathcal{V}_2(\mathcal{K})$ as well as every vertex of every edge in $\mathcal{V}_1(\mathcal{K})$ are contained in \mathcal{K} fullfilling the inclusion principle.

Example 2.2 (Real Life Simplicial Complex). *coauthorship graph? cannot find a nice picture*

 *find a natural example of the simplicial complex with an illustration*

Comparing to the definition of the hypergraph above, it is easy to see that simplicial complex is a special case of a hypergraph where every edge is enclosed with respect to the inclusion (every subset of every hyperedge is a hyperedge). In other words, simplicial complex contains additional structural rigidness which allows to formally describe the topology of \mathcal{K} ; as a result, one is specifically interested in the formal descrtiption of the nested inclusion principle achieved through *boundary operators* defined in the subsections below.

Prior to discussing boundary mappings, we briefly cover the algebraic structure of such operators known as *Hodge's theory*.

2.3 Hodge's Theory

Two linear operators A and B are said to satisfy Hodge's theory if and only if their composition is a null operator,


$$AB = 0 \tag{2.3}$$

which is equivalent to $\text{im } B \subseteq \ker A$.

Definition 2.3. For a pair of operators A and B satisfying Hodge's theory, the *quotient space* \mathcal{H} is defined as follows:

$$\mathcal{H} = \ker A /_{\text{im } B} \tag{2.4}$$

where each element of \mathcal{H} is a manifold $\mathbf{x} + \text{im } B = \{\mathbf{x} + \mathbf{y} \mid \forall \mathbf{y} \in \text{im } B\}$ for $\mathbf{x} \in \ker A$. It follows directly from the definition that \mathcal{H} is an abelian group under addition.

By [Definition 2.3](#), the quotient space \mathcal{H} is a collection  *in a general sense* of equivalence classes $\mathbf{x} + \text{im } B$. Then, each class $\mathbf{x} + \text{im } B = \mathbf{x}_H + \text{im } B$ for some $\mathbf{x}_H \perp \text{im } B$ (both $\mathbf{x}, \mathbf{x}_H \in \ker A$); indeed, since the orthogonal component \mathbf{x}_H (referred as *harmonic representative*) of \mathbf{x} with respect to $\text{im } B$ is unique, the map $\mathbf{x}_H \leftrightarrow \mathbf{x} + \text{im } B$ is bijectonal.

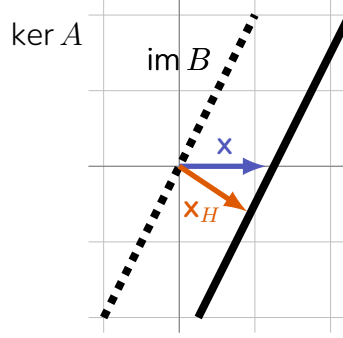


Figure 2.2: Illustration of a harmonic representative for an equivalence class

Theorem 2.4 ([1, Thm 5.3]). Let A and B be linear operators, $AB = 0$. Then the homology group \mathcal{H} satisfies:

$$\mathcal{H} = \ker A / \text{im } B \cong \ker A \cap \ker B^\top, \quad (2.5)$$

where \cong denotes the isomorphism²

Proof. One builds the isomorphism through the harmonic representative, as discussed above. It sufficient to note that $\mathbf{x}_H \perp \text{im } B \Leftrightarrow \mathbf{x}_H \in \ker B^\top$ in order to complete the proof. \square

Lemma 2.5 ([1, Thm 5.2]). Let A and B be linear operators, $AB = 0$. Then:

$$\ker A \cap \ker B^\top = \ker (A^\top A + BB^\top) \quad (2.6)$$

Proof. Note that if $\mathbf{x} \in \ker A \cap \ker B^\top$, then $\mathbf{x} \in \ker A$ and $\mathbf{x} \in \ker B^\top$, so $\mathbf{x} \in \ker (A^\top A + BB^\top)$. As a result, $\ker A \cap \ker B^\top \subset \ker (A^\top A + BB^\top)$.

On the other hand, let $\mathbf{x} \in \ker (A^\top A + BB^\top)$, then

$$A^\top A \mathbf{x} + BB^\top \mathbf{x} = 0 \quad (2.7)$$

Exploiting $AB = 0$ and multiplying the equation above by B^\top and A one gets the following:

$$\begin{aligned} B^\top BB^\top \mathbf{x} &= 0 \\ AA^\top A \mathbf{x} &= 0 \end{aligned} \quad (2.8)$$

²Two vector spaces V and W over the same field F are isomorphic if there is a bijection $T: V \mapsto W$ which preserves addition and scalar multiplication, that is, for all vectors $\mathbf{u}, \mathbf{v} \in V$ and all $c \in F$

$$T(\mathbf{u} + \mathbf{v}) = T(\mathbf{u}) + T(\mathbf{v}), \quad T(c\mathbf{v}) = cT(\mathbf{v})$$

Note that $AA^T A\mathbf{x} = 0 \Leftrightarrow A^T A\mathbf{x} \in \ker A$, but $A^T A\mathbf{x} \in \operatorname{im} A^T$, so by Fredholm alternative, $A^T A\mathbf{x} = 0$. Finally, for $A^T A\mathbf{x} = 0$:

$$A^T A\mathbf{x} = 0 \Rightarrow \mathbf{x}^T A^T A\mathbf{x} = 0 \iff \|A\mathbf{x}\|^2 = 0 \Rightarrow \mathbf{x} \in \ker A \quad (2.9)$$

Similarly, for the second equation, $\mathbf{x} \in \ker B^T$ which completes the proof. \square

 Here we need some words about the transitions.

Since $AB = 0$, $B^T A^T = 0$ or $\operatorname{im} A^T \subset \ker B^T$. Then, exploiting $\mathbb{R}^n = \ker A \oplus \operatorname{im} A^T$:

$$\begin{aligned} \ker B^T &= \ker B^T \cap \mathbb{R}^n = \ker B^T \cap (\ker A \oplus \operatorname{im} A^T) = \\ &= (\ker A \cap \ker B^T) \oplus (\operatorname{im} A^T \cap \ker B^T) \end{aligned} \quad (2.10)$$

Given [Lemma 2.5](#), $\ker A \cap \ker B^T = \ker (A^T A + BB^T)$ and, since $\operatorname{im} A^T \subset \ker B^T$, $\operatorname{im} A^T \cap \ker B^T = \operatorname{im} A^T$, yielding the decomposition of the whole space:

Theorem 2.6 (Hodge Decomposition). *Let A and B be linear operators, $AB = 0$. Then:*

$$\mathbb{R}^n = \overbrace{\operatorname{im} A^T \oplus \ker (A^T A + BB^T)}^{\ker B^T} \oplus \underbrace{\operatorname{im} B}_{\ker A} \quad (2.11)$$


2.4 Boundary and Laplacian Operators

2.4.1 Boundary operators B_k

Each simplicial complex \mathcal{K} has a nested structure of simplices: indeed, if σ is a simplex of order k , $\sigma \in \mathcal{V}_k(\mathcal{K})$, then all of $(k-1)$ -th order faces forming the boundary of σ also belong to \mathcal{K} : for instance, for the triangle $\{1, 2, 3\}$ all the border edges $\{1, 2\}$, $\{1, 3\}$ and $\{2, 3\}$ are also in the simplicial complex, [Figure 2.1](#).

This nested property implies that one can build a formal map from a simplex to its boundary enclosed inside the simplicial complex.

Definition 2.7 (Chain spaces). Let \mathcal{K} be a simplicial complex; then the space \mathcal{C}_k of formal sums of simplices from $\mathcal{V}_k(\mathcal{K})$ over real numbers is called a *k-th chain space*.

Chain spaces on its own are naturally present in the majority of the network models: \mathcal{C}_0 is a space of states of vertices (e.g. in the dynamical system $\dot{\mathbf{x}} = A\mathbf{x}$ the evolving vector $\mathbf{x} \in \mathcal{C}_0$), \mathcal{C}_1 — is a space of (unrestricted) flows on graphs edges, and so on  [refs?](#).

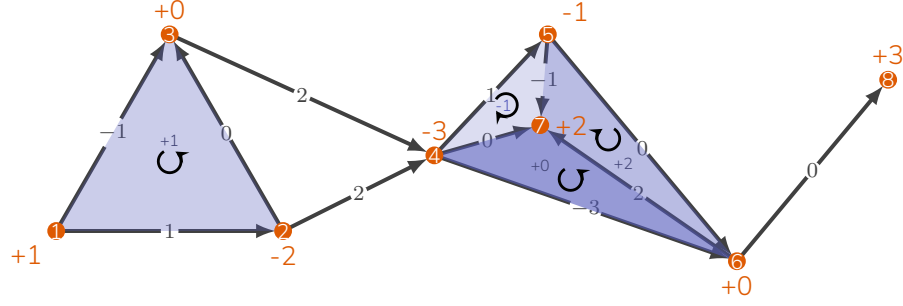


Figure 2.3: Example of chains on the simplicial complex

Example 2.3. We provide an example of chains from \mathcal{C}_0 , \mathcal{C}_1 and \mathcal{C}_2 in Figure 2.3:

$$\begin{aligned} \mathbf{c}_0 &= [1] - 2[2] - 3[4] - [5] + 2[7] + 3[8] \\ \mathbf{c}_1 &= [1, 2] - [1, 3] + 2[2, 4] + 2[3, 4] + [4, 5] - 3[4, 6] - [5, 7] + 2[6, 7] \\ \mathbf{c}_2 &= [1, 2, 3] - [4, 5, 7] + 2[5, 6, 7] \end{aligned} \quad (2.12)$$

Since \mathcal{C}_k is a linear space, the elements of $\mathcal{V}_k(\mathcal{K})$ is a natural basis of \mathcal{C}_k and $\mathcal{C}_k \cong \mathbb{R}^{m_k}$ with versor vectors forming the basis and corresponding to simplices in $\mathcal{V}_k(\mathcal{K})$. For instance, in Example 2.3:

$$\begin{aligned} \mathbf{c}_0 &= \begin{pmatrix} 1 & -2 & 0 & -3 & -1 & 0 & 2 & 3 \end{pmatrix}^\top \\ \mathbf{c}_1 &= \begin{pmatrix} 1 & -1 & 0 & 2 & 2 & 1 & -3 & 0 & -1 & 0 & 2 & 0 \end{pmatrix}^\top \\ \mathbf{c}_2 &= \begin{pmatrix} 1 & -1 & 0 & 2 \end{pmatrix}^\top \end{aligned} \quad (2.13)$$

For the matrix notation of any operator acting on chain spaces \mathcal{C}_k , it is natural to order simplices in $\mathcal{V}_k(\mathcal{K})$ in some fashion. Additionally, for a matter of bookkeeping one introduces the notion of *orientation* of each simplex in \mathcal{C}_k , e.g. for simplex $\sigma = [u_1, u_2, \dots, u_{k+1}]$ the orientation maybe be assigned as the permutation sign, $\text{sgn}(u_1, u_2, \dots, u_{k+1})$. We provide examples of oriented simplices in Figure 2.3 in case of the lexicographical orientation described above. Note that neither ordering of simplices or their orientation should not be able to substantially alter topological properties of the simplicial complex if defined correctly.

To form a boundary map, one aims to replicate the action of the operator on Figure 2.4: to map a simplex (f.i. $[1, 2, 3]$) to some combination of faces on its border (in case of Figure 2.4, $[1, 2]$, $[1, 3]$, $[2, 3]$). This implies that a boundary operator B_k should map \mathcal{C}_k onto \mathcal{C}_{k-1} . Formally,

Definition 2.8. Let \mathcal{K} be a simplicial complex with corresponding family of chain spaces \mathcal{C}_k . Then the action of a boundary map $B_k, B_k : \mathcal{C}_k \mapsto \mathcal{C}_{k-1}$, is defined as an alternating

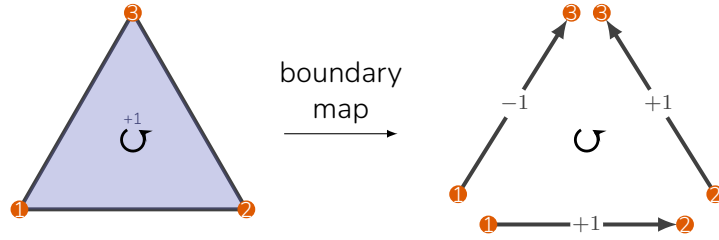


Figure 2.4: Sample action of the boundary operators

sum:

$$B_k[u_1, u_2, \dots, u_{k+1}] = \sum_{i=1}^{k+1} (-1)^i [u_1, u_2, \dots, u_{i-1}, u_{i+1}, \dots, u_{k+1}] \quad (2.14)$$

In the case of Figure 2.3,

$$B_2[1, 2, 3] = [1, 2] - [1, 3] + [2, 3] \quad (2.15)$$

The alternating nature of the definition upholds so called *fundamental lemma of homology* stating “the boundary of the boundary is zero”. Indeed,

$$B_1 B_2[1, 2, 3] = B_1([1, 2] - [1, 3] + [2, 3]) = [1] - [2] - [1] + [3] + [2] - [3] = 0 \quad (2.16)$$

Lemma 2.9 (Fundamental Lemma of Homology, FLH). *Let \mathcal{K} be a simplicial complex with corresponding boundary operators B_k . Then:*

$$B_k B_{k+1} = 0 \quad (2.17)$$

Proof. It is sufficient to directly calculate the action of the composition of B_k and B_{k+1} on $\sigma = [u_1, u_2, \dots, u_{k+2}]$:

$$\begin{aligned} B_k B_{k+1}[u_1, u_2, \dots, u_{k+2}] &= B_k \left(\sum_{i=1}^{k+2} (-1)^i [u_1, u_2, \dots, u_{i-1}, u_{i+1}, \dots, u_{k+2}] \right) = \\ &= \sum_{i=1}^{k+2} (-1)^i B_k[u_1, u_2, \dots, u_{i-1}, u_{i+1}, \dots, u_{k+2}] = \\ &= \sum_{i=1}^{k+2} (-1)^i \left(\sum_{j=1}^{i-1} (-1)^j [u_1, u_2, \dots, u_{j-1}, u_{j+1}, \dots, u_{i-1}, u_{i+1}, \dots, u_{k+2}] + \right. \\ &\quad \left. + \sum_{j=i+1}^{k+2} (-1)^{j-1} [u_1, u_2, \dots, u_{i-1}, u_{i+1}, \dots, u_{j-1}, u_{j+1}, \dots, u_{k+2}] \right) = \end{aligned} \quad (2.18)$$

$$\begin{aligned}
&= \sum_{i=1}^{k+2} \sum_{j=1}^{i-1} (-1)^{i+j} [u_1, u_2, \dots, u_{j-1}, u_{j+1}, \dots, u_{i-1}, u_{i+1}, \dots, u_{k+2}] + \\
&\quad - \sum_{i=1}^{k+2} \sum_{j=i+1}^{k+2} (-1)^{i+j} [u_1, u_2, \dots, u_{i-1}, u_{i+1}, \dots, u_{j-1}, u_{j+1}, \dots, u_{k+2}] = \\
&= \sum_{\substack{i,j=1 \\ j < i}}^{k+2} (-1)^{i+j} [u_1, u_2, \dots, u_{j-1}, u_{j+1}, \dots, u_{i-1}, u_{i+1}, \dots, u_{k+2}] + \\
&\quad - \sum_{\substack{i,j=1 \\ j > i}}^{k+2} (-1)^{i+j} [u_1, u_2, \dots, u_{i-1}, u_{i+1}, \dots, u_{j-1}, u_{j+1}, \dots, u_{k+2}] = 0
\end{aligned} \tag{2.19}$$

For the final nullification it is sufficient to notice that two terms coincide upon the interchange $i \leftrightarrow j$. \square

Since we already established basis in \mathcal{C}_k and \mathcal{C}_{k-1} via elements of $\mathcal{V}_k(\mathcal{K})$ and $\mathcal{V}_{k-1}(\mathcal{K})$ respectively, for the rest of the work we assume boundary operators B_k in the matrix form, $B_k \in \mathbb{R}^{m_{k-1} \times m_k}$, see an example in Figure 2.5. Matrices B_k are naturally sparse and are de facto oriented incidence matrices for higher-order structures; specifically, as seen on Figure 2.5, B_1 is known in the classical graph models as *incidence matrix*.

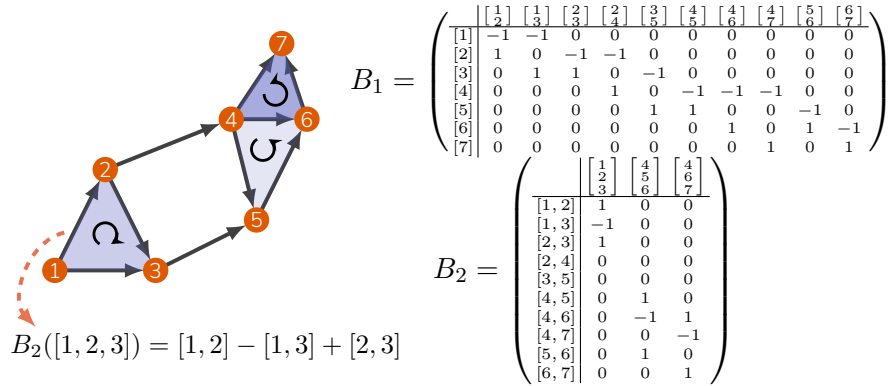


Figure 2.5: Left-hand side panel: example of simplicial complex \mathcal{K} on 7 nodes, and of the action of B_2 on the 2-simplex $[1, 2, 3]$; 2-simplices included in the complex are shown in red, arrows correspond to the orientation. Panels on the right: matrix forms B_1 and B_2 of boundary operators respectively.

2.4.2 Homology group and Hodge Laplacians L_k

2.4.2.1 Homology group as Quotient space

For a given simplicial complex \mathcal{K} , each pair of boundary maps B_k and B_{k+1} satisfy Hodge's theory due to the Fundamental Lemma of Homology, Lemma 2.9, which means



Figure 2.6: Continuous and analogous discrete manifolds with one 1-dimensional hole ($\dim \bar{\mathcal{H}}_1 = 1$). Left pane: the continuous manifold; center pane: the discretization with mesh vertices; right pane: a simplicial complex built upon the mesh. Triangles in the simplicial complex \mathcal{K} are colored gray (right).

that this special case of quotient space $\ker B_k / \text{im } B_{k+1}$ is correctly defined:

Definition 2.10 (Homology group). Let \mathcal{K} be a simplicial complex with corresponding boundary maps B_k . Then the quotient space:

$$\mathcal{H}_k = \ker B_k / \text{im } B_{k+1} \quad (2.20)$$

is referred as k -th *homology group* of the simplicial complex \mathcal{K} .

Homology group on its own is an object of a quite high level of abstraction which can be met in various areas of algebra. Instead, since \mathcal{H}_k connects simplices and their borders by definition, we exploit the very first definition of the homology group in the algebraic topology as way to define and categorize holes in the manifold.

Remark 2.11. [🔗 of holes and boudaries](#)

[🔗 refs](#)

Indeed, simplicial complex \mathcal{K} is not a manifold, although it may be seen as a discretization of the manifold, [Figure 2.6](#). Moreover, one can show the convergence of the discrete homology group \mathcal{H}_k to its continuous counterpart in case of $k = 1$ in thermodynamic limit, [🔗 refs](#).

2.4.2.2 Elements of the Hodge decomposition as harmonic/vorticity/potential flow

[🔗 Maybe we will need here a quick discussion with connection to the continuous case](#)

Similarly, simplicial complex-specific case of the Hodge's decomposition, [Theorem 2.6](#), holds:

$$\mathbb{R}^{m_k} = \overbrace{\text{im } B_k^\top \oplus \ker \left(B_k^\top B_k + B_{k+1} B_{k+1}^\top \right)}^{\ker B_{k+1}^\top} \oplus \text{im } B_{k+1} \quad (2.21)$$

$\underbrace{\hspace{10em}}_{\ker B_k}$

Definition 2.12 (Hodge Laplacian Operator). Let \mathcal{K} be a simplicial complex with corresponding boundary maps B_k . Then due to [Theorem 2.4](#) and [Lemma 2.5](#),

$$\mathcal{H}_k \cong \ker \left(B_k^\top B_k + B_{k+1} B_{k+1}^\top \right) \quad (2.22)$$

Operator $L_k = B_k^\top B_k + B_{k+1} B_{k+1}^\top$ is known as k -th *Hodge Laplacian* (or *higher-order Laplacian*) operator. Two terms $L_k^\downarrow = B_k^\top B_k$ and $L_k^\uparrow = B_{k+1} B_{k+1}^\top$ are known as k -th *down-* and *up-*Laplacians respectively.

As established above, the homology group $\mathcal{H}_k \cong \ker L_k$ consists of *harmonic representative* or *harmonic chains* (which name is explained by the fact of falling into the kernel of the corresponding Laplacian operator L_k). Elements of the remaining components of the decomposition can be described through the analogy with differential operator on simplicial complexes. For instance,

1. the conjugate boundary map B_1^\top is a discrete derivative on the graph: $B_1^\top[u_1, u_2] = [u_2] - [u_1]$, hence $B_1^\top = \text{grad}$ and $B_1 = -\text{div}$;
2. the conjugate boundary map B_2^\top is a discrete curl operator: $B_2^\top[u_1, u_2, u_3] = [u_1, u_2] - [u_1, u_3] + [u_2, u_3] = [u_1, u_2] + [u_2, u_3] + [u_3, u_1]$; note that the fundamental lemma of homology de facto restates a widely known fact $\text{curl grad} = 0$;
3. 1-st order Hodge Laplacian operator then can be rewritten as a composition of the differential operators:

$$L_1 = -\text{grad div} + \text{curl}^* \text{curl} = \Delta_1 \quad (2.23)$$

Operator Δ_1 is known as a *Helmholtzian operator on graphs*, an analogue of the vector Laplacian, [2].

Following this, the elements of $\text{im } B_1^\top = \text{im}(\text{grad})$ are referred as *potential flows* (since each element y_i of a vector $\mathbf{y} = B_1^\top \mathbf{x}$ is a difference of potentials between some pair nodes α and β forming the i -th edge); similarly, elements of $\text{im } B_2 = \text{im}(\text{curl}^*)$ are *vector potentials* or *vorticities*, and $\ker B_1$ and $\ker B_2^\top$ are divergence- and curl-free flows respectively (a more low level discussion of these two subspaces is provided further).

Remark 2.13. Consideration above provides a solid intuition but lacks clearly formality: indeed, in order to properly define graph's gradient, divergence and curl operators, one would need to discuss alternating functions on a graph (co-chains) and corresponding coboundary operator and cohomology, [1], and show a direct connection with discrete differential forms on manifolds. We choose to abstain from the introduction of another

quite abstract entity since it should not affect the clarity of the numerical analysis of the Laplacian operators conducted further.

2.4.2.3 Laplacian operators L_k

The k -th order Hodge Laplacian operator $L_k = B_k^\top B_k + B_{k+1} B_{k+1}^\top$ naturally joins the boundary relational information about simplices of different orders in \mathcal{K} and describes the topological structure of the complex.

In its matrix form, L_k is symmetric ($L_k^\top = L_k$) and semi-positive definite ($\mathbf{x}^\top L_k \mathbf{x} = \mathbf{x}^\top B_k^\top B_k \mathbf{x} + \mathbf{x}^\top B_{k+1} B_{k+1}^\top \mathbf{x} = \|B_k \mathbf{x}\|^2 + \|B_{k+1}^\top \mathbf{x}\|^2 \geq 0$) operator. Moreover, individual entries of down- and up-Laplacians L_k^\downarrow and L_k^\uparrow describe oriented adjacency of simplices in $\mathcal{V}_k(\mathcal{K})$. Namely, two simplices $\sigma, \sigma' \in \mathcal{V}_k(\mathcal{K})$ are down-adjacent by a common face $\tau \in \mathcal{V}_{k-1}(\mathcal{K})$ with a similar (so the orientation of a common face agrees or disagrees with the orientation of σ and σ' simultaneously) and dissimilar orientation (otherwise); analogously, one can define an upper-adjacent pair $\sigma, \sigma' \in \mathcal{V}_k(\mathcal{K})$ belonging to the same $\tau \in \mathcal{V}_{k+1}(\mathcal{K})$. Then

$$[L_k^\downarrow]_{ij} = \begin{cases} k+1, & \text{if } i = j \\ 1, & \text{if } i \neq j \text{ and } \sigma_i, \sigma_j \text{ are upper-adjacent with similar orientation} \\ -1, & \text{if } i \neq j \text{ and } \sigma_i, \sigma_j \text{ are upper-adjacent with dissimilar orientation} \\ 0 & \text{otherwise} \end{cases} \quad (2.24)$$

$$[L_k^\uparrow]_{ij} = \begin{cases} \deg(\sigma_i), & \text{if } i = j \\ 1, & \text{if } i \neq j \text{ and } \sigma_i, \sigma_j \text{ are down-adjacent with similar orientation} \\ -1, & \text{if } i \neq j \text{ and } \sigma_i, \sigma_j \text{ are down-adjacent with dissimilar orientation} \\ 0 & \text{otherwise} \end{cases} \quad (2.25)$$

where $\deg(\sigma_i)$ is the number of simplices in $\mathcal{V}_{k+1}(\mathcal{K})$ having σ_i as a face.

 figure?

2.4.2.4 Classical Laplacian and its kernel elements

Homology groups described above are not necessarily devoted to the case of higher-order interaction (or, equally, high order simplicial complexes \mathcal{K}). Indeed, the 0-order homology group is properly defined for 0-skeleton of any simplicial complex, or, in other words, the classical graph.

Assuming the absent boundary of a node, $B_0 = 0$, the 0-order Hodge Laplacian or classical graph Laplacian L_0 is defined as

$$L_0 = B_1 B_1^\top \quad \text{and} \quad \mathcal{H}_0 = \ker B_1^\top \quad (2.26)$$

2.4.2.5 Kernel elements of L_k

 Some relation to the continuous case

Spreading and balancing as a mechanism of the non-local circulation

2.5 Weighted and Normalised Boundary Operators

 definition and motivation of the weighting scheme

Note that, from the definition $\bar{B}_k = W_{k-1}^{-1} B_k W_k$ and (??), we immediately have that $\bar{B}_k \bar{B}_{k+1} = 0$. Thus, the group $\bar{\mathcal{H}}_k = \ker \bar{B}_k / \text{im } \bar{B}_{k+1}$ is well defined for any choice of positive weights w_k and is isomorphic to $\ker \bar{L}_k$. While the homology group may depend on the weights, we observe below that its dimension does not. Precisely, we have

Proposition 2.14. *The dimension of the homology groups of \mathcal{K} is not affected by the weights of its k -simplices. Precisely, if W_k are positive diagonal matrices, we have*

$$\dim \ker \bar{B}_k = \dim \ker B_k, \quad \dim \ker \bar{B}_k^\top = \dim \ker B_k^\top, \quad \dim \bar{\mathcal{H}}_k = \dim \mathcal{H}_k. \quad (2.27)$$

Moreover, $\ker B_k = W_k \ker \bar{B}_k$ and $\ker B_k^\top = W_{k-1}^{-1} \ker \bar{B}_k^\top$.

Proof. Since W_k is an invertible diagonal matrix,

$$\bar{B}_k \mathbf{x} = 0 \iff W_{k-1}^{-1} B_k W_k \vec{x} = 0 \iff B_k W_k \vec{x} = 0.$$

Hence, if $\vec{x} \in \ker \bar{B}_k$, then $W_k \vec{x} \in \ker B_k$, and, since W_k is bijective, $\dim \ker \bar{B}_k = \dim \ker B_k$. Similarly, one observes that $\dim \ker \bar{B}_k^\top = \dim \ker B_k^\top$.

Moreover, since $\bar{B}_k \bar{B}_{k+1} = 0$, then $\text{im } \bar{B}_{k+1} \subseteq \ker \bar{B}_k$ and $\text{im } \bar{B}_k^\top \subseteq \ker \bar{B}_{k+1}^\top$. This yields $\ker \bar{B}_k \cup \ker \bar{B}_{k+1}^\top = \mathbb{R}^{\mathcal{V}_k} = \ker B_k \cup \ker B_{k+1}^\top$. Thus, for the homology group it holds:

$$\begin{aligned} \dim \bar{\mathcal{H}}_k &= \dim \left(\ker \bar{B}_k \cap \ker \bar{B}_{k+1}^\top \right) = \\ &= \dim \ker \bar{B}_k + \dim \ker \bar{B}_{k+1}^\top - \dim \left(\ker \bar{B}_k \cup \ker \bar{B}_{k+1}^\top \right) = \\ &= \dim \ker B_k + \dim \ker B_{k+1}^\top - \dim \left(\ker B_k \cup \ker B_{k+1}^\top \right) = \dim \mathcal{H}_k \end{aligned}$$

□

 normalisation theorem

Chapter 3

Topological Stability as MNP

3.1 General idea of the topological stability

3.1.1 Alternative with a persistent homology



3.1.2 Transition to the spectral properties

3.2 101 on Spectral Matrix Nearness Problems

definition

Generally speaking, for a given matrix A a *matrix nearness problem* consists of finding the closest possible matrix X among the admissible set with a number of desired properties. For instance, one may search for the closest (in some metric) symmetric positive/negative definite matrix, unitary matrix or the closest graph Laplacian.

Motivated by the topological meaning of the *kernel* of Hodge Laplacians L_k , we assume the specific case of *spectral* MNPs: here one aims for the target matrix X to have a specific spectrum $\sigma(X)$. For instance in the stability study of the dynamical system $\dot{\mathbf{x}} = A\mathbf{x}$ one can search for the closest Hurwitz matrix such that $\text{Re}[\lambda_i] < 0$ for all $\lambda_i \in \sigma(X)$; similarly, assuming given matrix A is a graph Laplacian, one can search for the closest disconnected graph (so the algebraic connectivity $\lambda_2 = 0$).

Here we recite the optimization framework developed by REFREFREF  [fix it](#) for the class of the spectral matrix nearness problems; one should note, however, that this is by far not the only approach to the task, REFREFREF  [also fix it with Nicholas and others, I guess?](#).

3.2.1 Functional and Gradient Flow

Let us assume that $X = A + \Delta$ and instead of searching for X , we search for the perturbation matrix Δ ; additionally, we assume that Ω is the admissible set containing all possible perturbations Δ .

3.2.2 Transition to the gradient flow

 Derivative

3.2.3 Constraint gradient flow

3.2.4 Sparsity pattern and rank-1 optimizers

3.2.5 Idea of two level optimization

3.3 Direct approach: failure and discontinuity problems

3.3.1 Principal spectral inheritance

Before moving on to the next section, we recall here a relatively direct but important spectral property that connects the spectra of the k -th and $(k + 1)$ -th order Laplacians.

Theorem 3.1 (HOL's spectral inheritance). *Let L_k and L_{k+1} be higher-order Laplacians for the same simplicial complex \mathcal{K} . Let $\bar{L}_k = \bar{L}_k^{down} + \bar{L}_k^{up}$, where $\bar{L}_k^{down} = \bar{B}_k^\top \bar{B}_k$ and $\bar{L}_k^{up} = \bar{B}_{k+1} \bar{B}_{k+1}^\top$. Then:*

1. $\sigma_+(\bar{L}_k^{up}) = \sigma_+(\bar{L}_{k+1}^{down})$, where $\sigma_+(\cdot)$ denotes the positive part of the spectrum;
2. if $0 \neq \mu \in \sigma_+(\bar{L}_k^{up}) = \sigma_+(\bar{L}_{k+1}^{down})$, then the eigenvectors are related as follows:
 - (a) if \mathbf{x} is an eigenvector for \bar{L}_k^{up} with the eigenvalue μ , then $\mathbf{y} = \frac{1}{\sqrt{\mu}} \bar{B}_{k+1}^\top \mathbf{x}$ is an eigenvector for \bar{L}_{k+1}^{down} with the same eigenvalue;
 - (b) if \mathbf{u} is an eigenvector for \bar{L}_{k+1}^{down} with the eigenvalue μ and $\mathbf{u} \notin \ker \bar{B}_{k+1}$, then $\mathbf{v} = \frac{1}{\sqrt{\mu}} \bar{B}_{k+1} \mathbf{u}$ is an eigenvector for \bar{L}_k^{up} with the same eigenvalue;
3. for each Laplacian \bar{L}_k : if $\mathbf{v} \notin \ker \bar{L}_k^{down}$ is the eigenvector for \bar{L}_k^{down} , then $\mathbf{v} \in \ker \bar{L}_k^{up}$; vice versa, if $\mathbf{u} \notin \ker \bar{L}_k^{up}$ is the eigenvector for \bar{L}_k^{up} , then $\mathbf{v} \in \ker \bar{L}_k^{down}$;

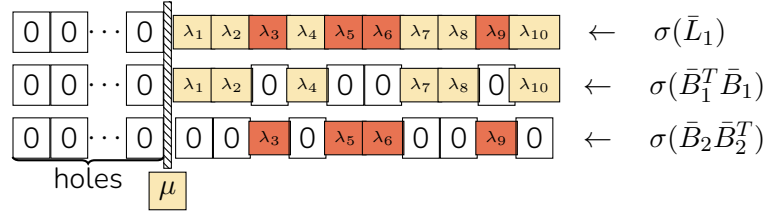


Figure 3.1: Illustration for the principal spectrum inheritance (Theorem 3.1) in case $k = 0$: spectra of \bar{L}_1 , \bar{L}_1^\downarrow and \bar{L}_1^\uparrow are shown. Colors signify the splitting of the spectrum, $\lambda_i > 0 \in \sigma(\bar{L}_1)$; all yellow eigenvalues are inherited from $\sigma_+(\bar{L}_0)$; red eigenvalues belong to the non-inherited part. Dashed barrier μ signifies the penalization threshold (see the target functional in ??) preventing homological pollution (see ??).

4. consequently, there exist $\mu \in \sigma_+(\bar{L}_k)$ with an eigenvector $\mathbf{u} \in \ker \bar{L}_k^{up}$, and $\nu \in \sigma_+(\bar{L}_{k+1})$ with an eigenvector $\mathbf{u} \in \ker \bar{L}_{k+1}^{down}$, such that:

$$\bar{B}_k^\top \bar{B}_k \mathbf{v} = \mu \mathbf{v}, \quad \bar{B}_{k+2} \bar{B}_{k+2}^\top \mathbf{u} = \nu \mathbf{u}.$$

Proof. For (2a) it is sufficient to note that $\bar{L}_{k+1}^{down} \mathbf{y} = \bar{B}_{k+1}^\top \bar{B}_{k+1} \frac{1}{\sqrt{\mu}} \bar{B}_{k+1}^\top \mathbf{x} = \frac{1}{\sqrt{\mu}} \bar{B}_{k+1}^\top \bar{L}_k^{up} \mathbf{x} = \sqrt{\mu} \bar{B}_{k+1}^\top \mathbf{x} = \mu \mathbf{y}$. Similarly, for (2b): $\bar{L}_k^{up} \mathbf{v} = \bar{B}_{k+1} \bar{B}_{k+1}^\top \frac{1}{\sqrt{\mu}} \bar{B}_{k+1} \mathbf{u} = \frac{1}{\sqrt{\mu}} \bar{B}_{k+1} \bar{L}_{k+1}^{down} \mathbf{u} = \mu \mathbf{v}$; joint 2(a) and 2(b) yield (1). Hodge decomposition immediately yields the strict separation of eigenvectors between \bar{L}_k^{up} and \bar{L}_k^{down} , (3); given (3), all the inherited eigenvectors from (2a) fall into the $\ker \bar{L}_{k+1}^{down}$, thus resulting into (4). \square

In other words, the variation of the spectrum of the k -th Laplacian when moving from one order to the next one works as follows: the down-term \bar{L}_{k+1}^{down} inherits the positive part of the spectrum from the up-term of \bar{L}_k^{up} ; the eigenvectors corresponding to the inherited positive part of the spectrum lie in the kernel of \bar{L}_{k+1}^{up} ; at the same time, the “new” up-term \bar{L}_{k+1}^{up} has a new, non-inherited, part of the positive spectrum (which, in turn, lies in the kernel of the $(k+2)$ -th down-term).

In particular, we notice that for $k = 0$, since $B_0 = 0$ and $\bar{L}_0 = \bar{L}_0^{up}$, the theorem yields $\sigma_+(\bar{L}_0) = \sigma_+(\bar{L}_1^{down}) \subseteq \sigma_+(\bar{L}_1)$. In other terms, the positive spectrum of the \bar{L}_0 is inherited by the spectrum of \bar{L}_1 and the remaining (non-inherited) part of $\sigma_+(\bar{L}_1)$ coincides with $\sigma_+(\bar{L}_1^{up})$. Figure 3.1 provides an illustration of the statement of Theorem 3.1 for $k = 0$.

3.3.2 Example with inherited disconnectedness

3.3.3 Example with faux edges (different weighting scheme)

3.4 Functional, derivative and alternating scheme

3.4.1 Target Functional

3.4.2 Free gradient calculation

Theorem 3.2 (Derivative of simple eigenvalues). *Consider a continuously differentiable path of square symmetric matrices $A(t)$ for t in an open interval \mathcal{I} . Let $\lambda(t)$, $t \in \mathcal{I}$, be a continuous path of simple eigenvalues of $A(t)$. Let $\vec{x}(t)$ be the eigenvector associated to the eigenvalue $\lambda(t)$ and assume $\|\vec{x}(t)\| = 1$ for all t . Then λ is continuously differentiable on \mathcal{I} with the derivative (denoted by a dot)*

$$\dot{\lambda} = \vec{x}^\top \dot{A} \vec{x} = \langle \vec{x} \vec{x}^\top, \dot{A} \rangle. \quad (3.1)$$

Moreover, “continuously differentiable” can be replaced with “analytic” in the assumption and the conclusion.

Let us denote the perturbed weight matrix by $\tilde{W}_1(t) = W_1 + \varepsilon E(t)$, and the corresponding $\tilde{W}_0(t) = W_0(\tilde{W}_1(t))$ and $\tilde{W}_2(t) = W_2(\tilde{W}_1(t))$, defined accordingly as discussed in Section ???. From now on we omit the time dependence for the perturbed matrices to simplify the notation. Since \tilde{W}_0 , \tilde{W}_1 and \tilde{W}_2 are necessarily diagonal, by the chain rule we have $\dot{\tilde{W}}_i(t) = \varepsilon \text{diag} \left(J_1^i \dot{E} \vec{1} \right)$, where $\vec{1}$ is the vector of all ones, $\text{diag}(\vec{v})$ is the diagonal matrix with diagonal entries the vector \vec{v} , and J_1^i is the Jacobian matrix of the i -th weight matrix with respect to \tilde{W}_1 , which for any $u_1 \in \mathcal{V}_1$ and $u_2 \in \mathcal{V}_i$, has entries $[J_1^i]_{u_1, u_2} = \frac{\partial}{\partial \tilde{w}_1(u_1)} \tilde{w}_i(u_2)$.

Next, in the following two lemmas, we express the time derivative of the Laplacian \bar{L}_0 and \bar{L}_1^{up} as functions of $E(t)$. The proofs of these results are straightforward and omitted for brevity. In what follows, $\text{Sym}[A]$ denotes the symmetric part of the matrix A , namely $\text{Sym}[A] = (A + A^\top)/2$.

Lemma 3.3 (Derivative of \bar{L}_0). *For the simplicial complex \mathcal{K} with the initial edges' weight matrix W_1 and fixed perturbation norm ε , let $E(t)$ be a smooth path and $\tilde{W}_0, \tilde{W}_1, \tilde{W}_2$ be corresponding perturbed weight matrices. Then,*

$$\frac{1}{2\varepsilon} \frac{d}{dt} \bar{L}_0(t) = \tilde{W}_0^{-1} B_1 \tilde{W}_1 \dot{E} B_1^\top \tilde{W}_0^{-1} - \text{Sym} \left[\tilde{W}_0^{-1} \text{diag} \left(J_1^0 \dot{E} \vec{1} \right) \bar{L}_0 \right]. \quad (3.2)$$

Lemma 3.4 (Derivative of \bar{L}_1^{up}). *For the simplicial complex \mathcal{K} with the initial edges' weight matrix W_1 and fixed perturbation norm ε , let $E(t)$ be a smooth path and $\tilde{W}_0, \tilde{W}_1, \tilde{W}_2$ be corresponding perturbed weight matrices. Then,*

$$\frac{1}{2\varepsilon} \frac{d}{dt} \bar{L}_1^{up}(t) = -\text{Sym} \left[\tilde{W}_1^{-1} B_2 \tilde{W}_2^2 B_2^\top \tilde{W}_1^{-1} \dot{E} \tilde{W}_1^{-1} \right] + \tilde{W}_1^{-1} B_2 \tilde{W}_2 \text{diag} \left(J_1^0 \dot{E} \bar{1} \right) B_2^\top \tilde{W}_1^{-1}$$

Combining Lemma 3.2 with Lemma 3.3 and Lemma 3.4 we obtain the following expression for the free gradient of the functional.

Theorem 3.5 (The free gradient of $F(\varepsilon, E)$). *Assume the initial weight matrices W_0, W_1 and W_2 , as well as the parameters $\varepsilon > 0$, $\alpha > 0$ and $\mu > 0$, are given. Additionally assume that $E(t)$ is a differentiable matrix-valued function such that the first non-zero eigenvalue $\lambda_+(\varepsilon, E)$ of $\bar{L}_1^{up}(\varepsilon, E)$ and the second smallest eigenvalue $\mu_2(\varepsilon, E)$ of $\bar{L}_0(\varepsilon, E)$ are simple. Let $\tilde{W}_0, \tilde{W}_1, \tilde{W}_2$ be corresponding perturbed weight matrices; then:*

$$\begin{aligned} \frac{1}{\varepsilon} \nabla_E F(\varepsilon, E)(t) = & \lambda_+(\varepsilon, E) \cdot \\ & \cdot \left[\text{Sym} \left[-\tilde{W}_1^{-1} B_2 \tilde{W}_2^2 B_2^\top \tilde{W}_1^{-1} \vec{x}_+ \vec{x}_+^\top \tilde{W}_1^{-1} \right] \right. \\ & + \text{diag} \left(J_1^{2^\top} \text{diagvec} \left(B_2^\top \tilde{W}_1^{-1} \vec{x}_+ \vec{x}_+^\top \tilde{W}_1^{-1} B_2 \tilde{W}_2 \right) \right) \left. - \frac{\alpha}{\mu} \max \left\{ 0, 1 - \frac{\mu_2(\varepsilon, E)}{\mu} \right\} \right] \\ & \cdot \left[B_1^\top \tilde{W}_0^{-1} \vec{y}_2 \vec{y}_2^\top \tilde{W}_0^{-1} B_1 \tilde{W}_1 - \text{diag} \left(J_1^{0^\top} \text{diagvec} \left(\text{Sym}[\tilde{W}_0^{-1} \vec{y}_2 \vec{y}_2^\top \bar{L}_0] \right) \right) \right] \end{aligned}$$

where \vec{x}_+ is a unit eigenvector of \bar{L}_1^{up} corresponding to λ_+ , \vec{y}_2 is a unit eigenvector of \bar{L}_0 corresponding to μ_2 , and the operator $\text{diagvec}(X)$ returns the main diagonal of X as a vector.

Proof. To derive the expression for the gradient $\nabla_E F$, we exploit the chain rule for the time derivative: $\dot{\lambda} = \langle \frac{d}{dt} A(E(t)), \vec{x} \vec{x}^\top \rangle = \langle \nabla_E \lambda, \dot{E} \rangle$. Then it is sufficient to apply the cyclic perturbation for the scalar products of Lemma 3.3 and Lemma 3.4 with $\vec{x}_+ \vec{x}_+^\top$ and $\vec{y}_2 \vec{y}_2^\top$ respectively. The final transition requires the formula:

$$\langle A, \text{diag}(B E \bar{1}) \rangle = \langle \text{diag} \left(B^\top (\text{diagvec } A) \right), E \rangle.$$

□

Remark 3.6. The derivation above assumes the simplicity of both $\mu_2(\varepsilon, E)$ and $\lambda_+(\varepsilon, E)$. This assumption is not restrictive as simplicity for these extremal eigenvalues is a generic property. Indeed we observe simplicity in all our numerical tests.

3.4.3 The constrained gradient system and its stationary points

In this section we are deriving from the free gradient determined in Theorem 3.5 the constrained gradient of the considered functional, that is the projected gradient (with respect to the Frobenius inner product) onto the manifold $\Omega \cap \Pi_\varepsilon$, which consists of perturbations E of unit norm which preserve the structure of W .

In order to obtain the constrained gradient system, we need to project the unconstrained gradient given by Theorem 3.5 onto the feasible set and also to normalize E to preserve its unit norm. Using the Karush-Kuhn-Tucker conditions on a time interval where the set of 0-weight edges remain unchanged, the projection is done via the mapping $\mathbb{P}_+G(\varepsilon, E)$, where

$$[\mathbb{P}_+X]_{ij} = \begin{cases} X_{ij}, & [W_1 + \varepsilon E]_{ij} > 0 \\ 0, & \text{otherwise} \end{cases}.$$

Further, in order to comply with the constraint $\|E(t)\|^2 = 1$, we must have

$$0 = \frac{1}{2} \frac{d}{dt} \|E(t)\|^2 = \langle E(t), \dot{E}(t) \rangle. \quad (3.3)$$

Thus, we obtain the following constrained optimization problem for the admissible direction of the steepest descent

Lemma 3.7 (Direction of steepest admissible descent). *Let $E, G \in \mathbb{R}^{m \times m}$ with G given by (??), and $\|E\| = 1$. On a time interval where the set of 0-weight edges remains unchanged, the gradient system reads*

$$\dot{E}(t) = -\mathbb{P}_+G(\varepsilon, E(t)) + \kappa \mathbb{P}_+E(t), \quad \text{where} \quad \kappa = \frac{\langle \varepsilon, G(E(t)), \mathbb{P}_+E(t) \rangle}{\|\mathbb{P}_+E(t)\|^2}. \quad (3.4)$$

Proof. We need to orthogonalize $\dot{E}(t)$ with respect to $E(t)$. To this end, we introduce a linear orthogonality correction, i.e. we set $\dot{E} = \mathbb{P}_+(-G - \kappa E)$, and we determine κ by imposing the constraint $\langle E, \dot{E} \rangle = 0$. We then have

$$0 = \langle E, \dot{E} \rangle = \langle E, \mathbb{P}_+(-G - \kappa E) \rangle = -\langle \mathbb{P}_+E, G \rangle - \kappa \langle \mathbb{P}_+E, \mathbb{P}_+E \rangle,$$

and the result follows. □

Equation (3.4) suggests that the system goes “primarily” in the direction of the antigradient $-G(\varepsilon, E)$, thus the functional is expected to decrease along it.

Lemma 3.8 (Monotonicity). *Let $E(t)$ of unit Frobenius norm satisfy the differential equation (3.4), with G given by (??). Then, $F(\varepsilon, E(t))$ decreases monotonically with t .*

Proof. We consider first the simpler case where the non-negativity projection does not apply so that $G = G(\varepsilon, E)$ (without \mathbb{P}_+). Then

$$\begin{aligned} \frac{d}{dt}F(\varepsilon, E)(t) &= \left\langle \nabla_E F_k(\varepsilon, E), \dot{E} \right\rangle = \langle \varepsilon G(\varepsilon, E(t)), -G(\varepsilon, E(t)) + \kappa E(t) \rangle \\ &= -\varepsilon \|G(\varepsilon, E)\|^2 + \varepsilon \frac{\langle G(\varepsilon, E), E \rangle}{\langle E, E \rangle} \langle G(\varepsilon, E), E \rangle \\ &= \varepsilon \left(-\|G(\varepsilon, E)\|^2 + \frac{|\langle G(\varepsilon, E), E \rangle|^2}{\|E\|^2} \right) \leq 0 \end{aligned} \quad (3.5)$$

where the final estimate is given by the Cauchy-Bunyakovsky-Schwarz inequality. The derived inequality holds on the time interval without the change in the support of \mathbb{P}_+ (so that no new edges are prohibited by the non-negativity projection). \square

3.4.4 Constrained gradient

3.4.5 Alternating scheme

3.4.6 Implementation

3.4.6.1 Algorithms

3.4.6.2 Computation of the first non-zero eigenvalue

3.4.6.3 Preconditioning in the eigen-phase

3.5 Benchmarking

3.5.1 Illustrative Example

We consider here a small example of a simplicial complex \mathcal{K} of order 2 consisting of eight 0-simplices (vertices), twelve 1-simplices (edges), four 2-simplices $\mathcal{V}_2 = \{[1, 2, 3], [1, 2, 8], [4, 5, 6], [5, 6, 7]$ and one corresponding hole $[2, 3, 4, 5]$, hence, $\beta_1 = 1$. By design, the dimensionality of the homology group $\bar{\mathcal{H}}_1$ can be increased only by eliminating edges $[1, 2]$ or $[5, 6]$; for the chosen weight profile $w_1([1, 2]) > w_1([5, 6])$, hence, the method should converge to the minimal perturbation norm $\varepsilon = w_1([5, 6])$ by eliminating the edge $[5, 6]$, Figure 3.2.

The exemplary run of the optimization framework in time is shown on Figure 3.3. The top panel of Figure 3.3 provides the continued flow of the target functional $F(\varepsilon, E(t))$ consisting of the initial α -phase (in green) and alternated constrained (in blue) and free

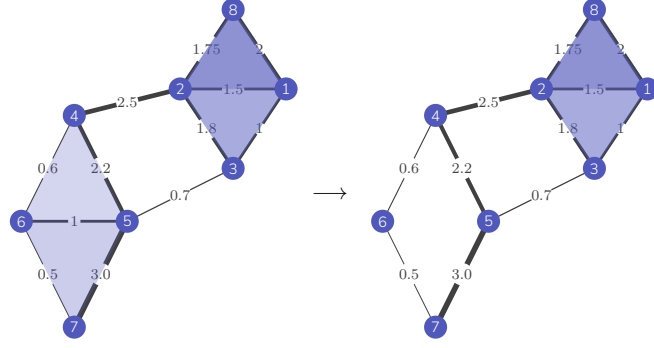


Figure 3.2: Simplicial complex \mathcal{K} on 8 vertices for the illustrative run (on the left): all 2-simplices from \mathcal{V}_2 are shown in blue, the weight of each edge $w_1(e_i)$ is given on the figure. On the right: perturbed simplicial complex \mathcal{K} through the elimination of the edge $[5, 6]$ creating additional hole $[5, 6, 7, 8]$.

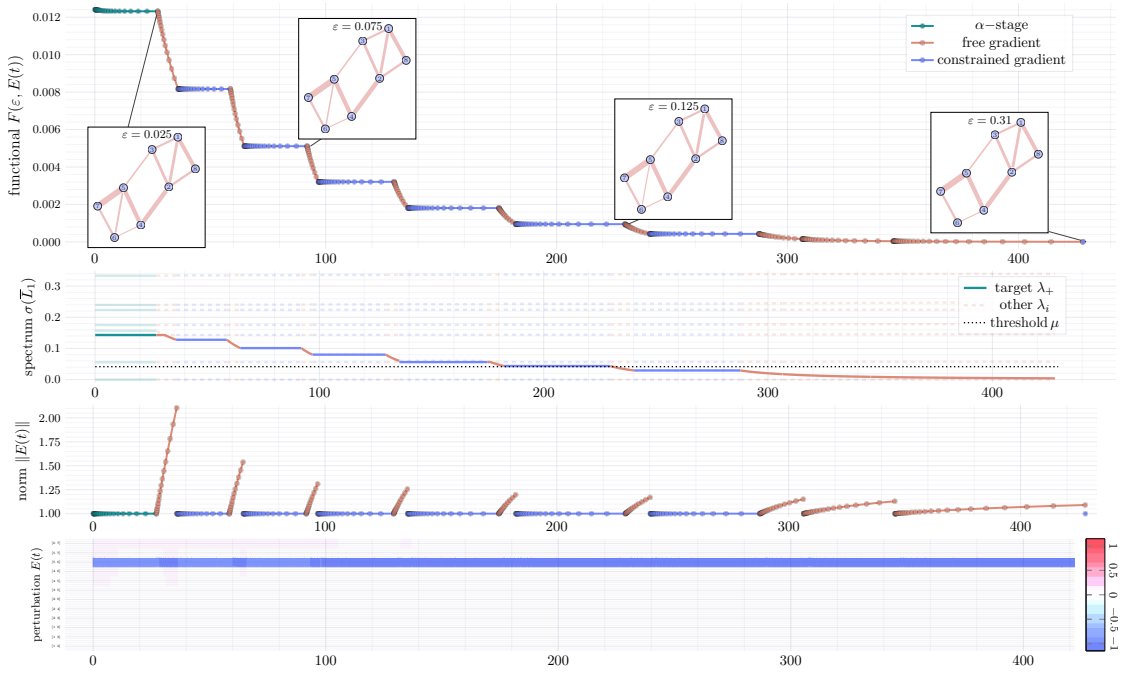


Figure 3.3: Illustrative run of the framework determining the topological stability: the top pane — the flow of the functional $F(\varepsilon, E(t))$; the second pane — the flow of $\sigma(\bar{L}_1)$, λ_+ is highlighted; third pane — the change of the perturbation norm $\|E(t)\|$; the bottom pane — the heatmap of the perturbation profile $E(t)$.

gradient (in orange) stages. As stated above, $F(\varepsilon, E(t))$ is strictly monotonic along the flow since the support of \mathbb{P}_+ does not change. Since the initial setup is not pathological with respect to the connectivity, the initial α -phase essentially reduces to a single constrained gradient flow and terminates after one run with $\alpha = \alpha_*$. The constrained gradient stages are characterized by a slow changing $E(t)$, which is essentially due to the flow performing small adjustments to find the correct rotation on the unit sphere, whereas the free gradient stage quickly decreases the target functional.

The second panel shows the behaviour of first non-zero eigenvalue $\lambda_+(\varepsilon, E(t))$ (solid

line) of $\bar{L}_1^{up}(\varepsilon, E(t))$ dropping through the ranks of $\sigma(\bar{L}_1(\varepsilon, E(t)))$ (semi-transparent); similar to the case of the target functional $F(\varepsilon, E(t))$, $\lambda_+(\varepsilon, E(t))$ monotonically decreases. The rest of the eigenvalues exhibit only minor changes, and the rapidly changing λ_+ successfully passes through the connectivity threshold μ (dotted line).

The third and the fourth panels show the evolution of the norm of the perturbation $\|E(t)\|$ and the perturbation $E(t)$ itself, respectively. The norm $\|E(t)\|$ is conserved during the constrained-gradient and the α - stages; these stages correspond to the optimization of the perturbation shape, as shown by the small positive values at the beginning of the bottom panel which eventually vanish. During the free gradient integration the norm $\|E(t)\|$ increases, but the relative change of the norm declines with the growth of ε_i to avoid jumping over the smallest possible ε . Finally, due to the simplicity of the complex, the edge we want to eliminate, 56, dominates the flow from the very beginning (see bottom panel); such a clear pattern persists only in small examples, whereas for large networks the perturbation profile is initially spread out among all the edges.

3.5.2 Triangulation Benchmark

To provide more insight into the computational behavior of the method, we synthesize here an almost planar graph dataset. Namely, we assume N uniformly sampled vertices on the unit square with a network built by the Delaunay triangulation; then, edges are randomly added or erased to obtain the sparsity ν (so that the graph has $\frac{1}{2}\nu N(N-1)$ edges overall). An order-2 simplicial complex $\mathcal{K} = (\mathcal{V}_0, \mathcal{V}_1, \mathcal{V}_2)$ is then formed by letting \mathcal{V}_0 be the generated vertices, \mathcal{V}_1 the edges, and \mathcal{V}_2 every 3-clique of the graph; edges' weights are sampled uniformly between $1/4$ and $3/4$, namely $w_1(e_i) \sim U[\frac{1}{4}, \frac{3}{4}]$.

An example of such triangulation is shown in Figure 3.4a; here $N = 8$ and edges $[6, 8]$ and $[2, 7]$ were eliminated to achieve the desired sparsity.

We sample networks with a varying number of vertices $N = 10, 16, 22, 28$ and varying sparsity pattern $\nu = 0.35, 0.5$ which determine the number of edges in the output as $m = \nu \frac{N(N-1)}{2}$. Due to the highly randomized procedure, topological structures of a sampled graph with a fixed pair of parameters may differ substantially, so 10 networks with the same (N, ν) pair are generated. For each network, the working time (without considering the sampling itself) and the resulted perturbation norm ε , and are reported in Figure 3.4b and Figure 3.4c, respectively. As anticipated in Section ??, we show the performance of two implementations of the method, one based on LSMR and one based on LSMR preconditioned by using the incomplete Cholesky factorization of the initial matrices. We observe that,

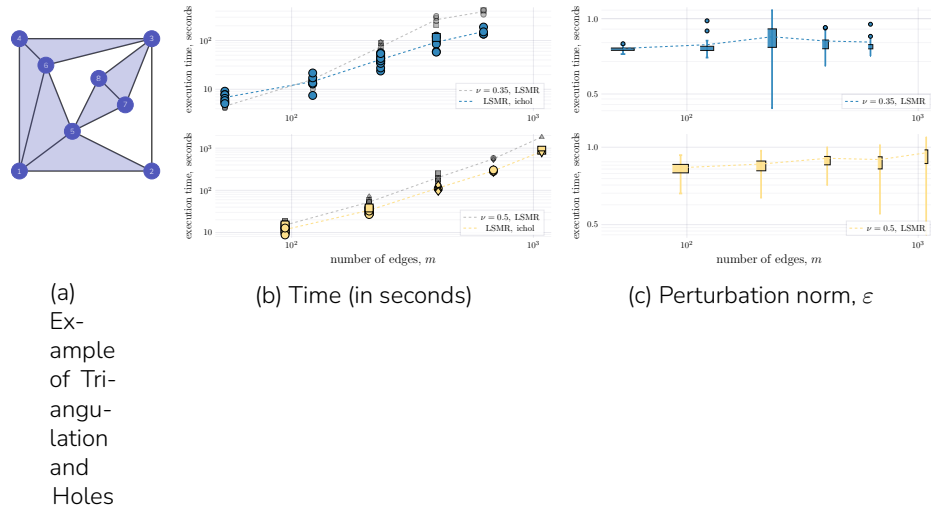


Figure 3.4: Benchmarking Results on the Synthetic Triangulation Dataset: varying sparsities $\nu = 0.35, 0.5$ and $N = 16, 22, 28, 34, 40$; each network is sampled 10 times. Shapes correspond to the number of eliminated edges in the final perturbation: 1 : \circ , 2 : \square , 3 : \diamond , 4 : \triangle . For each pair (ν, N) , the un-preconditioned and Cholesky-preconditioned execution times are shown.

- the computational cost of the whole procedure lies between $\mathcal{O}(m^2)$ and $\mathcal{O}(m^3)$
- denser structures, with a higher number of vertices, result in the higher number of edges being eliminated; at the same time, even most dense cases still can exhibit structures requiring the elimination of a single edge, showing that the flow does not necessarily favor multi-edge optima;
- the required perturbation norm ϵ is growing with the size of the graph, Figure 3.4c, but not too fast: it is expected that denser networks would require larger ϵ to create a new hole; at the same time if the perturbation were to grow drastically with the sparsity ν , it would imply that the method tries to eliminate sufficiently more edges, a behavior that resembles convergence to a sub-optimal perturbation;
- preconditioning with a constant incomplete Cholesky multiplier, computed for the initial Laplacians, provides a visible execution time gain for medium and large networks. Since the quality of the preconditioning deteriorates as the flow approaches the minimizer (as a non-zero eigenvalue becomes 0), it is worth investigating the design of a preconditioner for the up-Laplacian that can be efficiently updated.

3.5.3 Transportation Networks

Finally, we provide an application to real-world examples based on city transportation networks. We consider networks for Bologna, Anaheim, Berlin Mitte, and Berlin Tiergarten; each network consists of nodes — intersections/public transport stops — connected by edges (roads) and subdivided into zones; for each road the free flow time, length, speed limit are known; moreover, the travel demand for each pair of nodes is provided through the dataset of recorded trips. All the datasets used here are publicly available at <https://github.com/bstabler/TransportationNetworks>; Bologna network is provided by the Physic Department of the University of Bologna (enriched through the Google Maps API <https://developers.google.com/maps>).

The regularity of city maps naturally lacks 3-cliques, hence forming the simplicial complex based on triangulations as done before frequently leads to trivial outcomes. Instead, here we “lift” the network to city zones, thus more effectively grouping the nodes in the graph. Specifically:

1. we consider the completely connected graph where the nodes are zones in the city/region;
2. the free flow time between two zones is temporarily assigned as a weight of each edge: the time is as the shortest path between the zones (by the classic Dijkstra algorithm) on the initial graph;
3. similarly to what is done in the filtration used for persistent homology, we filter out excessively distant nodes; additionally, we exclude the longest edges in each triangle in case it is equal to the sum of two other edges (so the triangle is degenerate and the trip by the longest edge is always performed through to others);
4. finally, we use the travel demand as an actual weight of the edges in the final network; travel demands are scaled *logarithmically* via the transformation $w_i \mapsto \log_{10} \left(\frac{w_i}{0.95 \min w_i} \right)$; see the example on the left panel of Figure 3.5.

Given the definition of weights in the network, high instability (corresponding to small perturbation norm ε) implies structural phenomena around the “almost-hole”, where the faster and shorter route is sufficiently less demanded.

In the case of Bologna, Figure 3.5, the algorithm eliminates the edge [11, 47] (Casalecchio di Reno – Pianoro) creating a new hole $6 - 11 - 57 - 47$. We also provide examples of the eigenflows in the kernel of the Hodge Laplacian (original and additional perturbed): original eigenvectors correspond to the circulations around holes $7 - 26 - 12 - 20$ and $8 - 21 - 20 - 16 - 37$ non-locally spread in the neighborhood [?].

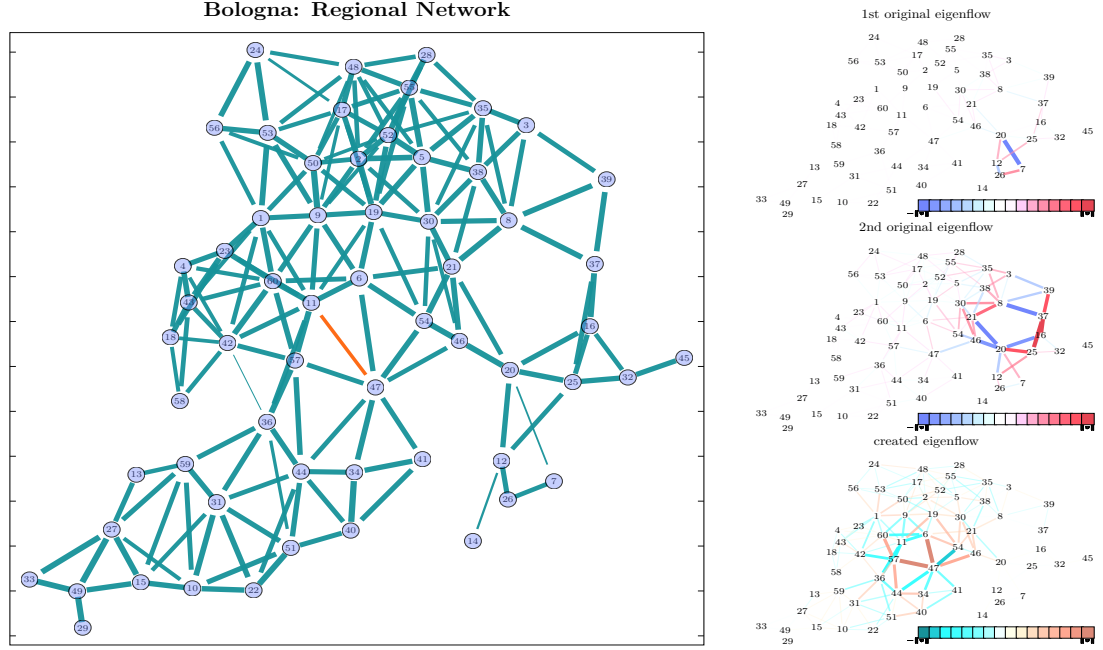


Figure 3.5: Example of the Transportation Network for Bologna. Left pane: original zone graph where the width of edges corresponds to the weight, to-be-eliminated edge is colored in red. Right pane: eigenflows, original and created; color and width correspond to the magnitude of entries.

| Cities | network | | | β_1 | logarithmic weights | | |
|-------------------|---------|-------|-------|-----------|--|---------------|--------|
| | m_0 | m_1 | m_2 | | time | ε | p |
| Bologna | 60 | 175 | 171 | 2 | 2.43s [11, 47] (4^{th} smallest) | 0.65 | 0.003 |
| Anaheim | 38 | 159 | 221 | 1 | 5.39s [10, 29] (11^{th} smallest) | 0.57 | 0.003 |
| Berlin-Tiergarten | 26 | 63 | 55 | 0 | 2.46s [6, 16] (20^{th} smallest) | 1.18 | 0.015 |
| Berlin-Mitte | 98 | 456 | 900 | 1 | 127s [57, 87] (6^{th}), [58, 87], (17^{th}) | 0.887 | 0.0016 |

Table 3.1: Topological instability of the transportation networks: filtered zone networks with the corresponding perturbation norm ε and its percentile among $w_1(\cdot)$ profile. For each simplicial complex the number of nodes, edges and triangles in $\mathcal{V}_2(\mathcal{K})$ are provided alongside the initial number of holes β_1 . The results of the algorithm consist of the perturbation norm, ε , computation time, and approximate percentile p .

The results for four different networks are summarized in the Table 3.1; p mimics the percentile, $\varepsilon / \sum_{e \in \mathcal{V}_1} w_i(e)$, showing the overall small perturbation norm contextually. At the same time, we emphasize that except Bologna (which is influenced by the geographical topology of the land), the algorithm does not choose the smallest weight possible; indeed, given our interpretation of the topological instability, the complex for Berlin-Tiergarten is stable and the transportation network is effectively constructed.

Chapter 4

Preconditioning

 Here we need to say general words about how we need an efficient preconditioning scheme.

4.1 Preconditioning 101

4.1.1 why do we care about the condition number?

4.1.2 Iterative methods

4.1.3 CG and convergence

 CGLS

4.1.4 Zoo of preconditioners

 Reinforced diagonal

 Cholesky  Incomplete Cholesky

4.2 LSq problem for the whole Laplacian -> up-Laplacian

4.3 Preconditioning on the up-Laplacian

4.3.1 Sparsification (Spielman/Osting)

4.3.2 Cholesky preconditioning for classical graphs

4.3.2.1 Stochastic Cholesky preconditioning

4.3.2.2 Schur complements

4.3.3 Problem with Schur complements in the case of L_1

 [Transition to collapsibility](#)

4.4 Collapsible simplicial complexes

4.4.1 Classical collapsibility

In this section we borrow the terminology from [3]; additionally, let us assume that considered simplicial complex \mathcal{K} is restricted to its 2-skeleton, so \mathcal{K} consists only of nodes, edges, and triangles, $\mathcal{K} = \mathcal{V}_0(\mathcal{K}) \cup \mathcal{V}_1(\mathcal{K}) \cup \mathcal{V}_2(\mathcal{K})$.

Simplex $\tau \in \mathcal{K}$ is called an (inclusion-wise) maximal face of simplex $\sigma \in \mathcal{K}$ if τ is maximal by inclusion simplex such that $\sigma \subseteq \tau$ and $\text{ord}(\sigma) < \text{ord}(\tau)$. For instance, in [Figure 4.1](#)

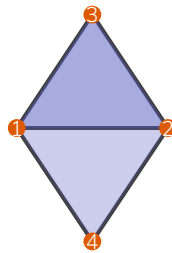


Figure 4.1: Example of a simplicial complex: free simplices and maximal faces.

the edge $\{1, 2\}$ and nodes $\{1\}$ and $\{2\}$ have two maximal faces, $\{1, 2, 3\}$ and $\{1, 2, 4\}$, while all the other edges and nodes have unique maximal faces — their corresponding triangles. Note that in the case of the node $\{1\}$, there are bigger simplices containing it besides the triangles (e.g. the edge $\{1, 2\}$), but they are not maximal by inclusion.

Definition 4.1 (Free simplex). The simplex $\sigma \in \mathcal{K}$ is free if it has exactly one maximal face τ , $\tau = \tau(\sigma)$. F.i. edges $\{1, 3\}$, $\{1, 4\}$, $\{2, 3\}$ and $\{2, 4\}$ are all free in Figure 4.1.

The collapse $\mathcal{K} \setminus \{\sigma\}$ of \mathcal{K} at a free simplex σ is the transition from the original simplicial complex \mathcal{K} to a smaller simplicial complex \mathcal{L} without the free simplex σ and the corresponding maximal face τ , $\mathcal{K} \rightarrow \mathcal{K}' = \mathcal{K} - \sigma - \tau$; namely, one can eliminate a simplex τ if it has an accessible (not included in another simplex) face σ .

Naturally, one can perform several consequent collapses at $\Sigma = \{\sigma_1, \sigma_2, \dots\}$ assuming σ_i is free in collapse simplicial complex from the previous stage; Σ is called the collapsing sequence. Formally:

Definition 4.2 (Collapsing sequence). Let \mathcal{K} be a simplicial complex. $\Sigma = \{\sigma_1, \sigma_2, \dots\}$ is a collapsing sequence if σ_1 is free in \mathcal{K} and each σ_i , $i > 1$, is free at $\mathcal{K}^{(i)} = \mathcal{K}^{(i-1)} \setminus \{\sigma_i\}$, $\mathcal{K}^{(1)} = \mathcal{K}$. The collapse of \mathcal{K} to a new complex \mathcal{L} at Σ is denoted by $\mathcal{L} = \mathcal{K} \setminus \Sigma$.

By the definition, every collapsing sequence Σ has a corresponding sequence $\mathbb{T} = \{\tau(\sigma_1), \tau(\sigma_2), \dots\}$ of maximal faces being collapsed at every step.

Definition 4.3 (Collapsible simplicial complex, [3]). The simplicial complex \mathcal{K} is collapsible if there exists a collapsing sequence Σ such that \mathcal{K} collapses to a single vertex at Σ , $\mathcal{K} \setminus \Sigma = \{v\}$.

Determining whether the complex is collapsible is in general *NP-complete*, [4], but can be almost linear for a set of specific families of \mathcal{K} , e.g. if the simplex can be embedded into the triangulation of the d -dimensional unit sphere, [5]. Naturally restricting the collapses to the case of d -collapses (such that $\text{ord}(\sigma)_i \leq d - 1$), one arrive at the notion of d -collapsibility, [6].

Definition 4.4 (d -Core). A d -Core is a subcomplex of \mathcal{K} such that every simplex of order $d - 1$ belongs to at least 2 simplices of order d . E.g. 2-Core is such a subcomplex of the original 2-skeleton \mathcal{K} that every edge from $\mathcal{V}_1(\mathcal{K})$ belong to at least 2 triangles from $\mathcal{V}_2(\mathcal{K})$.

Lemma 4.5 ([7]). \mathcal{K} is d -collapsible if and only if it does not contain a d -core.

Proof. The proof of the lemma above naturally follows from the definition of the core. Assume Σ is a d -collapsing sequence, and $\mathcal{K} \setminus \Sigma$ consists of more than a single vertex and has no free simplices of order $\leq d - 1$ ("collapsing sequence gets stuck"). Then, each simplex of order $d - 1$ is no free but belongs to at least 2 simplices of order d , so $\mathcal{K} \setminus \Sigma$ is a d -Core.

Conversely if a d -Core exists in the complex, the collapsing sequence should necessarily include its simplices of order $d - 1$ which can not become free during as a result of a sequence of collapses. Indeed, for σ from d -Core, $\text{ord}(\sigma) = d - 1$, to become free, one needs to collapse at least one of σ 's maximal faces for d -Core, all of whose faces are, in turn, contained in the d -Core (since d -Core is a simplicial complex). As a result one necessarily needs a prior collapse inside the d -Core to perform the first collapse in the d -Core, which is impossible. \square

In the case of the classical graph model, the 1-Core is a subgraph where each vertex has a degree at least 2; in other words, 1-Core cannot be a tree and necessarily contains a simple cycle. Hence, the collapsibility of a classical graph coincides with the acyclicity. The d -Core is the generalization of the cycle for the case of 1-collapsibility of the classical graph; additionally, the d -Core is very dense due to its definition. In the case of 2-Core, we provide simple exemplary structures on Figure 4.2 which imply various possible configurations for a d -Core, $d \geq 2$, hence a search for d -Core inside \mathcal{K} is neither trivial, no computationally cheap.

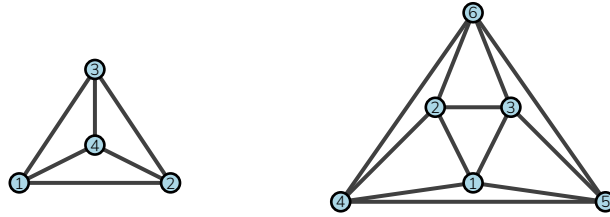


Figure 4.2: 2-Core, examples.

Additionally, we demonstrate that an arbitrary simplicial complex \mathcal{K} tends to contain 2-Cores as long as \mathcal{K} is denser than a trivially collapsible case. Assume the complex formed by triangulation of m_0 random points on the unit square with a sparsity pattern ν ; the triangulation itself with the corresponding ν_Δ is collapsible, but a reasonably small addition of edges already creates a 2-Core (since it is local), Figure 4.3, left. Similarly, sampled sensor networks, where $\exists \sigma \in \mathcal{V}_1(\mathcal{K}) : \sigma = [v_1, v_2] \iff \|v_1 - v_2\|_2 < \varepsilon$ for a chosen percolation parameter $\varepsilon > 0$, quickly form a 2-Core upon the densifying of the network.

However, in the following, we observe that a weaker condition is enough to efficiently design a preconditioner for any “sparse enough” simplicial complex.

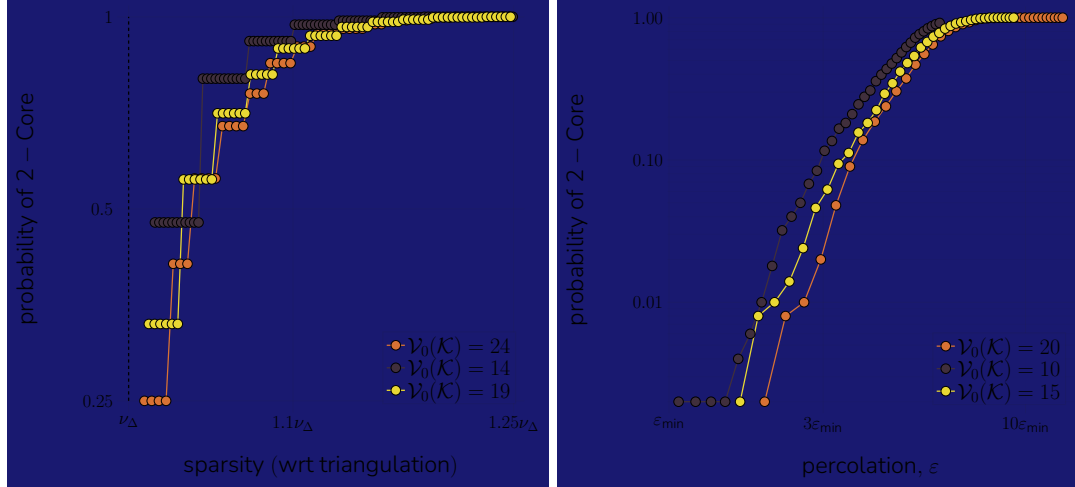


Figure 4.3: The probability of the 2-Core in richer-than-triangulation simplicial complexes: triangulation of random points modified to have $\left\lceil \nu \frac{|\mathcal{V}_0(\mathcal{K})| \cdot (|\mathcal{V}_0(\mathcal{K})| - 1)}{2} \right\rceil$ edges on the left; random sensor networks with ε -percolation on the right. ν_Δ defines the initial sparsity of the triangulated network; $\varepsilon_{\min} = \mathbb{E} \min_{x,y \in [0,1]^2} \|x - y\|_2$ is the minimal possible percolation parameter.

4.4.2 Weak collapsibility

Let the complex \mathcal{K} be restricted up to its 2-skeleton, $\mathcal{K} = \mathcal{V}_0(\mathcal{K}) \cup \mathcal{V}_1(\mathcal{K}) \cup \mathcal{V}_2(\mathcal{K})$, and \mathcal{K} is collapsible. Then the collapsing sequence Σ necessarily involves collapses at simplices σ_i of different orders: at edges (eliminating edges and triangles) and at vertices (eliminating vertices and edges). One can show that for a given collapsing sequence Σ there is a reordering $\tilde{\Sigma}$ such that $\dim \tilde{\sigma}_i$ are non-increasing, [5, Lemma 2.5]. Namely, if such a complex is collapsible, then there is a collapsible sequence $\Sigma = \{\Sigma_1, \Sigma_0\}$ where Σ_1 contains all the collapses at edges first and Σ_0 is composed of collapses at vertices. Note that the partial collapse $\mathcal{K} \setminus \Sigma_1 = \mathcal{L}$ eliminates all the triangles in the complex, $\mathcal{V}_2(\mathcal{L}) = \emptyset$; otherwise, the whole sequence Σ is not collapsing \mathcal{K} to a single vertex. Since $\mathcal{V}_2(\mathcal{L}) = \emptyset$, the associated up-Laplacian $L_1^\uparrow(\mathcal{L}) = 0$.

Definition 4.6 (Weakly collapsible complex). Simplicial complex \mathcal{K} restricted to its 2-skeleton is called *weakly collapsible*, if there exists a collapsing sequence Σ_1 such that the simplicial complex $\mathcal{L} = \mathcal{K} \setminus \Sigma_1$ has no simplices of order 2, $\mathcal{V}_2(\mathcal{L}) = \emptyset$ and $L_1^\uparrow(\mathcal{L}) = 0$.

Example 4.1. Note that a collapsible complex is necessarily weakly collapsible; the opposite does not hold. Consider the following example in Figure 4.4: the initial complex is weakly collapsible either by a collapse at $[3, 4]$ or at $[2, 4]$. After this, the only available collapse is at the vertex $[4]$ leaving the uncollapsible 3-vertex structure.

Theorem 4.7. Weak collapsibility of 2-skeleton \mathcal{K} is polynomially solvable.

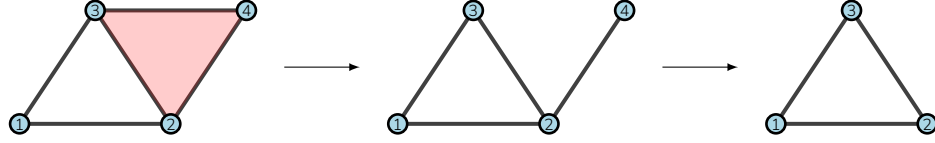


Figure 4.4: Example of weakly collapsible but not collapsible simplicial complex

Proof. The *greedy algorithm* for the collapsing sequence intuitively operates as follows: at each iteration perform any of possible collapses; in the absence of free edges, the complex should be considered not collapsible, [Algorithm 1](#). Clearly, such an algorithm runs polynomially with respect to the number of simplexes in \mathcal{K} .

The failure of the greedy algorithm indicates the existence of a weakly collapsible complex \mathcal{K} such that the greedy algorithm gets stuck at a 2-Core, which is avoidable for another possible order of collapses. Among all the counter exemplary complexes, let \mathcal{K} be a minimal one with respect to the number of triangles m_2 . Then there exist a free edge $\sigma \in \mathcal{V}_1(\mathcal{K})$ such that $\mathcal{K} \setminus \{\sigma\}$ is *collapsible* and another $\sigma' \in \mathcal{V}_2(\mathcal{K})$ such that $\mathcal{K} \setminus \{\sigma'\}$ is *not collapsible*.

Note that if \mathcal{K} is minimal then for any pair of free edges σ_1 and σ_2 belong to the same triangle: $\tau(\sigma_1) = \tau(\sigma_2)$. Indeed, for any $\tau(\sigma_1) \neq \tau(\sigma_2)$, $\mathcal{K} \setminus \{\sigma_1, \sigma_2\} = \mathcal{K} \setminus \{\sigma_2, \sigma_1\}$. Let $\tau(\sigma_1) \neq \tau(\sigma_2)$ for at least one pair of σ_1 and σ_2 ; in our assumption, either both $\mathcal{K} \setminus \{\sigma_1\}$ and $\mathcal{K} \setminus \{\sigma_2\}$, only $\mathcal{K} \setminus \{\sigma_1\}$ or none are collapsible. In the former case either $\mathcal{K} \setminus \{\sigma_1\}$ or $\mathcal{K} \setminus \{\sigma_2\}$ is a smaller example of the complex satisfying the assumption, hence, violating the minimality. If only $\mathcal{K} \setminus \{\sigma_1\}$ is collapsible, then $\mathcal{K} \setminus \{\sigma_2, \sigma_1\}$ is not collapsible; hence, $\mathcal{K} \setminus \{\sigma_1, \sigma_2\}$ is not collapsible, so $\mathcal{K} \setminus \{\sigma_1\}$ is a smaller example of a complex satisfying the assumption. Finally, if both $\mathcal{K} \setminus \{\sigma_1\}$ and $\mathcal{K} \setminus \{\sigma_2\}$ are collapsible, then for known σ' such that $\mathcal{K} \setminus \{\sigma'\}$ is not collapsible, $\tau(\sigma') \neq \tau(\sigma_1)$ or $\tau(\sigma') \neq \tau(\sigma_2)$, which revisits the previous point.

As a result, for σ ($\mathcal{K} \setminus \{\sigma\}$ is collapsible) and for σ' ($\mathcal{K} \setminus \{\sigma'\}$ is not collapsible) it holds that $\tau(\sigma) = \tau(\sigma') \Rightarrow \sigma \cap \sigma' = \{v\}$, so after collapses $\mathcal{K} \setminus \{\sigma\}$ and $\mathcal{K} \setminus \{\sigma'\}$ we arrive at two identical simplicial complexes modulo the hanging vertex irrelevant for the weak collapsibility. A simplicial complex can not be simultaneously collapsible and not collapsible, so the question of weak collapsibility can always be resolved by the greedy algorithm which has polynomial complexity. \square

4.4.3 Computational cost of the greedy algorithm

Let \mathcal{K} be a 2-skeleton; let Δ_σ be a set of triangles of \mathcal{K} containing the edge σ , $\Delta_\sigma = \{t \mid t \in \mathcal{V}_2(\mathcal{K}) \text{ and } \sigma \in t\}$. Then the edge σ is free iff $|\Delta_\sigma| = 1$ and $F = \{\sigma \mid |\Delta_\sigma| = 1\}$ is a

set of all free edges. Note that $|\Delta_e| \leq m_0 - 2 = \mathcal{O}(m_0)$.

Algorithm 1 GREEDY_COLLAPSE(\mathcal{K}): greedy algorithm for the weak collapsibility

Require: initial set of free edges F , adjacency sets $\{\Delta_{\sigma_i}\}_{i=1}^{m_1}$

```

1:  $\Sigma = [], \mathbb{T} = []$  ▷ initialize the collapsing sequence
2: while  $F \neq \emptyset$  and  $\mathcal{V}_2(\mathcal{K}) \neq \emptyset$  do
3:    $\sigma \leftarrow \text{pop}(F), \tau \leftarrow \tau(\sigma)$  ▷ pick a free edge  $\sigma$ 
4:    $\mathcal{K} \leftarrow \mathcal{K} \setminus \{\sigma\}, \Sigma \leftarrow [\Sigma \ \sigma], \mathbb{T} \leftarrow [\mathbb{T} \ \tau]$  ▷  $\tau$  is a triangle being collapsed;
    $\tau = [\sigma, \sigma_1, \sigma_2]$ 
5:    $\Delta_{\sigma_1} \leftarrow \Delta_{\sigma_1} \setminus \tau, \Delta_{\sigma_2} \leftarrow \Delta_{\sigma_2} \setminus \tau$  ▷ remove  $\tau$  from adjacency lists
6:    $F \leftarrow F \cup \{\sigma_i \mid i = 1, 2 \text{ and } |\Delta_{\sigma_i}| = 1\}$  ▷ update  $F$  if any of  $\sigma_1$  or  $\sigma_2$  has become free
7: end while
8: return  $\mathcal{K}, \Sigma, \mathbb{T}$ 

```

The complexity of [Algorithm 1](#) rests upon the precomputed $\sigma \mapsto \Delta_\sigma$ structure that de-facto coincides with the boundary operator B_2 (assuming B_2 is stored as a sparse matrix, the adjacency structure describes its non-zero entries). Similarly, the initial F set can be computed alongside the construction of B_2 matrix. Another concession is needed for the complexity of the removal of elements from Δ_{σ_i} and F , which may vary from $\mathcal{O}(1)$ on average up to guaranteed $\log(|\Delta_{\sigma_i}|)$. As a result, given a pre-existing B_2 operator, [Algorithm 1](#) runs linearly, $\mathcal{O}(m_1)$, or almost linearly depending on the realisation, $\mathcal{O}(m_1 \log m_1)$.

 [Picture](#)

4.5 HeCS preconditioning

Given ??, a weakly collapsible simplicial complex \mathcal{K} immediately yields an exact Cholesky decomposition for its up-Laplacian:

Lemma 4.8. *Assume \mathcal{K} , 2-skeleton simplicial complex, is weakly collapsible though the collapsing sequence Σ with the corresponding sequence of maximal faces \mathbb{T} . Let $B_2 W_2$ be a weighted boundary operator for \mathcal{K} . Then*

$$C = P_\Sigma B_2 W_2 P_\mathbb{T} \quad \text{is an exact Cholesky multiplier for} \quad P_\Sigma L_1^\uparrow(\mathcal{K}) P_\Sigma^\top,$$

i.e. $P_\Sigma L_1^\uparrow(\mathcal{K}) P_\Sigma^\top = C C^\top$, where P_Σ and $P_\mathbb{T}$ are permutation matrices for each sequence ($[P_\Sigma]_{ij} = 1 \iff j = \sigma_i$).

Proof. Note that the sequences Σ and \mathbb{T} (and the multiplication by the corresponding permutation matrices) impose only the reordering of $\mathcal{V}_1(\mathcal{K})$ and $\mathcal{V}_2(\mathcal{K})$ respectively; after such reordering the i -th edge collapses the i -triangle. Hence, the first $(i - 1)$ entries of

the i -th columns of the matrix $B_2 W_2$ ($[B_2 W_2]_{\cdot i} = \sqrt{w(t_i)} \mathbf{e}_{t_i}$) are zeros, otherwise one of the previous edges is not free. As a result, C is lower-triangular and by the direct computation $CC^\top = P_\Sigma L_1^\uparrow(\mathcal{K}) P_\Sigma^\top$. \square

An arbitrary simplicial complex \mathcal{K} is generally not weakly collapsible (see Figure 4.2). Specifically, weak collapsibility is a property of sparse simplicial complexes with the sparsity being measured by the number of triangles m_2 (in the weakly collapsible case $m_2 < m_1$); hence, the removal of triangles from $\mathcal{V}_2(\mathcal{K})$ can potentially destroy the 2-Core structure inside \mathcal{K} and make the complex weakly collapsible.

As a result, the original ?? may be reduced to the search for a collapsible subcomplex \mathcal{L} inside the original complex \mathcal{K} , in order to use an exact Cholesky multiplier of \mathcal{L} as an approximate Cholesky preconditioner for $L_1^\uparrow(\mathcal{K})$. Specifically:

Problem 1. Let \mathcal{K} be a 2-skeleton simplicial complex, $\mathcal{K} = \mathcal{V}_0(\mathcal{K}) \cup \mathcal{V}_1(\mathcal{K}) \cup \mathcal{V}_2(\mathcal{K})$ with the corresponding triangle weight matrix $W_2(\mathcal{K})$. Find the subcomplex \mathcal{L} such that:

- (1) it has the same set of 0- and 1-simplices, $\mathcal{V}_0(\mathcal{L}) = \mathcal{V}_0(\mathcal{K})$ and $\mathcal{V}_1(\mathcal{L}) = \mathcal{V}_1(\mathcal{K})$;
- (2) triangles in \mathcal{L} are subsampled, $\mathcal{V}_2(\mathcal{L}) \subseteq \mathcal{V}_2(\mathcal{K})$;
- (3) \mathcal{L} has the same 1-homology as \mathcal{K} ;
- (4) \mathcal{L} is weakly collapsible through some collapsing sequence Σ and corresponding sequence of maximal faces \mathbb{T} ;
- (5) the Cholesky multiplier $C = P_\Sigma B_2(\mathcal{L}) W_2(\mathcal{L}) P_\mathbb{T}$ improves the conditionality of $L_1^\uparrow(\mathcal{K})$:

$$\kappa_+(L_1^\uparrow(\mathcal{K})) \gg \kappa_+(C^\dagger P_\Sigma L_1^\uparrow(\mathcal{K}) P_\Sigma^\top C^{\dagger\top})$$

Conditions (1) and (2) imply that a subcomplex \mathcal{L} is obtained from \mathcal{K} through the elimination of triangles.

Remark 4.9 (On the conservation of the 1-homology). Since one transitions between the systems $L_1^\uparrow(\mathcal{K})\mathbf{x} = \mathbf{f}$ and $(C^\dagger P_\Sigma L_1^\uparrow(\mathcal{K}) P_\Sigma^\top C^{\dagger\top}) C^\top P_\Sigma \mathbf{x} = C^\dagger P_\Sigma \mathbf{f}$, it is necessary to have $\ker C^\top = \ker L_1^\uparrow(\mathcal{K}) = \ker W_2 B_2^\top$ so the transition is bijective (assuming $\mathbf{x} \perp \ker L_1^\uparrow(\mathcal{K})$).

Due to ?? and the spectral inheritance principle, [?, Thm. 2.7], $\ker L_k^\uparrow(\mathcal{X}) = \ker L_k(\mathcal{X}) \oplus B_k^\top \cdot \text{im } L_{k-1}^\uparrow$. The second part, $B_k^\top \cdot \text{im } L_{k-1}^\uparrow$, consists of the action of B_k^\top on non-zero related eigenvectors of L_{k-1}^\uparrow and is not dependent on $\mathcal{V}_{k+1}(\mathcal{K})$ (triangles, in case $k = 1$), hence remains conserved in the subcomplex from Problem 1. As a result, the conservation of 1-homology is sufficient to converse the kernels $\ker L_1^\uparrow(\mathcal{K}) = \ker L_1^\uparrow(\mathcal{L})$. Moreover, one can show that the subcomplex \mathcal{L} can only extend the kernel: $\ker L_1(\mathcal{K}) \subseteq \ker L_1(\mathcal{L})$.

Indeed, the elimination of the triangle $t \in \mathcal{V}_2(\mathcal{K})$ lifts the restriction $\mathbf{e}_t^\top \mathbf{x} = 0$ for $\mathbf{x} \in \ker L_1(\mathcal{K})$; hence, if $\mathbf{x} \in \ker L_1(\mathcal{K})$, then $\mathbf{x} \in \ker L_1(\mathcal{L})$.

Definition 4.10 (Subsampling matrix). Assume \mathcal{K} be a 2-skeleton simplicial complex; let \mathbb{T} be a subset of triangles, $\mathbb{T} \subset \mathcal{V}_2(\mathcal{K})$ (so forming the subcomplex $\mathcal{L} = \mathcal{V}_0(\mathcal{K}) \cup \mathcal{V}_1(\mathcal{K}) \cup \mathbb{T}$). Then Π is a subsampling matrix if

- Π is diagonal;
- $(\Pi)_{ii} = 1 \iff i \in \mathbb{T}$; otherwise, $(\Pi)_{ii} = 0$.

Lemma 4.11 (Optimal weight choice for the subcomplex). Let \mathcal{K} be a simplicial complex and \mathcal{L} be its subcomplex, satisfying [Problem 1](#), with fixed corresponding subsampling matrix Π . Then in order to obtain the closest up-Laplacian $L_1^\uparrow(\mathcal{L})$ to the original $L_1^\uparrow(\mathcal{K})$, one should choose the weight matrix $W_2(\mathcal{L})$ as follows:

$$W_2(\mathcal{L}) = W_2(\mathcal{K})\Pi$$

Proof. Let $W_2^2(\mathcal{K}) = W$; then $L_1^\uparrow(\mathcal{K}) = B_2 W B_2^\top$. Then $\widehat{W}\Pi$ is the diagonal matrix of weights of subsampled triangles (in case $t \notin \mathbb{T}$, the entry $(\widehat{W}\Pi)_{tt} = 0$). Note that $\Pi\widehat{W} = \widehat{W}\Pi = \Pi\widehat{W}\Pi$; then, ignoring the reordering of the edges, $L_1^\uparrow(\mathcal{L}) = B_2 \Pi \widehat{W} \Pi B_2^\top$ barring several zero columns and rows corresponding to some of the eliminated triangles.

Generally speaking, weights \widehat{W} of sampled triangles \mathbb{T} differ from the original weights W . Let $\widehat{W} = W + \Delta W$, where ΔW is still diagonal, but entries are not necessarily positive. Then one can formulate the question of the optimal weight redistribution as the optimization problem:

$$\min_{\Delta W} \left\| L_1^\uparrow(\mathcal{L}) - L_1^\uparrow(\mathcal{K}) \right\| = \min_{\Delta W} \left\| B_2 [\Pi(W + \Delta W)\Pi - W] B_2^\top \right\|$$

Let $\Delta W = \Delta W(t)$ where t is a virtual time parametrization; then one can compute the gradient $\nabla_{\Delta W} \sigma_1 \left(L_1^\uparrow(\mathcal{L}) - L_1^\uparrow(\mathcal{K}) \right)$ through the time derivative $\frac{d}{dt} \sigma_1 \left(L_1^\uparrow(\mathcal{L}) - L_1^\uparrow(\mathcal{K}) \right)$:

$$\begin{aligned} \dot{\sigma}_1 &= \mathbf{x}^\top B_2 \Pi \Delta \dot{W} \Pi B_2^\top \mathbf{x} = \left\langle B_2 \Pi \Delta \dot{W} \Pi B_2^\top, \mathbf{x} \mathbf{x}^\top \right\rangle = \text{Tr} \left(B_2 \Pi \Delta \dot{W} \Pi B_2^\top \mathbf{x} \mathbf{x}^\top \right) = \\ &= \left\langle \Pi B_2^\top \mathbf{x} \mathbf{x}^\top B_2 \Pi, \Delta \dot{W} \right\rangle = \left\langle \nabla_{\Delta W} \sigma_1, \Delta \dot{W} \right\rangle \end{aligned}$$

By projecting onto the diagonal structure of the weight perturbation,

$$\nabla_{\text{diag } \Delta W} \sigma_1 = \text{diag} \left(\Pi B_2^\top \mathbf{x} \mathbf{x}^\top B_2 \Pi \right).$$

Note that $\text{diag} \left(\Pi B_2^\top \mathbf{x} \mathbf{x}^\top B_2 \Pi \right)_{ii} = |\Pi B_2^\top \mathbf{x}|_i^2$; then the stationary point is characterized by $\Pi B_2^\top \mathbf{x} = 0 \iff \mathbf{x} \in \ker L_1^\uparrow$. The latter is impossible since \mathbf{x} is the eigenvector

corresponding to the largest eigenvalue; hence, since $\Pi(W + \Delta W)\Pi \neq W$, the optimal perturbation is $\Delta W \equiv 0$. \square

Remark 4.12. Given [Problem 1](#) and the optimal conserved triangle wait from [Theorem 4.11](#), one aims to preserve the kernel of subsampled Laplacian

$$\ker(B_2 W_2 \Pi W_2 B_2^\top) = \ker(B_2 W_2^2 B_2^\top)$$

Since $\Pi = \Pi^2$, $\ker L_1^\dagger = \ker W_2 B_2^\top$ and $\ker(B_2 W_2 \Pi W_2 B_2^\top) = \ker(\Pi W_2 B_2^\top)$. Additionally, $\ker W_2 B_2^\top \subseteq \ker(\Pi W_2 B_2^\top)$, so $\ker(B_2 W_2 \Pi W_2 B_2^\top) \neq \ker(B_2 W_2^2 B_2^\top) \iff$ there exists $\mathbf{y} \in \text{im } W_2 B_2^\top$ such that $W_2 B_2^\top \mathbf{y} \neq 0$ and $W_2 B_2^\top \mathbf{y} \in \ker \Pi$. Then in order to preserve the kernel, one needs $\text{im } W_2 B_2^\top \cap \ker \Pi = \{0\}$.

Theorem 4.13 (Conditionality of the Subcomplex). *Let \mathcal{L} be a weakly collapsible subcomplex of \mathcal{K} defined by the subsampling matrix Π and let C be a Cholesky multiplier of $L_1^\dagger(\mathcal{L})$ defined as in [Theorem 4.8](#). Then the conditioning of the symmetrically preconditioned L_1^\dagger is given by:*

$$\kappa_+(C^\dagger P_\Sigma L_1^\dagger P_\Sigma^\top C^{\top\dagger}) = \left(\kappa_+ \left((S_1 V_1^\top \Pi)^\dagger S_1 \right) \right)^2 = (\kappa_+(\Pi V_1))^2,$$

where V_1 forms the orthonormal basis of $\text{im } W_2 B_2^\top$.

Proof. By [Theorem 4.11](#), $W_2(\mathcal{L}) = \Pi W_2$; then let us consider the lower-triangular preconditioner $C = P_\Sigma B_2 W_2 \Pi P_\mathbb{T}$ for $P_\Sigma L_1^\dagger P_\Sigma^\top$; then the preconditioned matrix is given by:

$$\begin{aligned} C^\dagger (P_\Sigma L_1^\dagger P_\Sigma^\top) C^{\top\dagger} &= (P_\Sigma B_2 W_2 \Pi P_\mathbb{T})^\dagger (P_\Sigma L_1^\dagger P_\Sigma^\top) (P_\Sigma B_2 W_2 \Pi P_\mathbb{T})^{\top\dagger} = \\ &= P_\mathbb{T}^\top (B_2 W_2 \Pi)^\dagger L_1^\dagger (B_2 W_2 \Pi)^{\top\dagger} P_\mathbb{T} \end{aligned}$$

Note that $P_\mathbb{T}$ is unitary, so $\kappa_+(P_\mathbb{T} X P_\mathbb{T}^\top) = \kappa_+(X)$, hence the principle matrix is $(B_2 W_2 \Pi)^\dagger L_1^\dagger (B_2 W_2 \Pi)^{\top\dagger} (B_2 W_2 \Pi)^\dagger (B_2 W_2) (B_2 W_2)^\top (B_2 W_2 \Pi)^{\top\dagger}$. Since $\kappa_+(X^\top X) = \kappa_+^2(X)$, then in fact one needs to consider

$$\kappa_+((B_2 W_2 \Pi)^\dagger (B_2 W_2))$$

Let us consider the SVD-decomposition for $B_2 W_2 = U S V^\top$; more precisely,

$$B_2 W_2 = U S V^\top = \begin{pmatrix} U_1 & U_2 \end{pmatrix} \begin{pmatrix} S_1 & 0 \\ 0 & 0 \end{pmatrix} \begin{pmatrix} V_1^\top \\ V_2^\top \end{pmatrix} = U_1 S_1 V_1^\top$$

where S_1 is a diagonal invertible matrix. Note that U and U_1 have orthonormal columns and S_1 is diagonal and invertible, so

$$(B_2 W_2 \Pi)^\dagger B_2 W_2 = (S V^\top \Pi)^\dagger S V^\top = (S_1 V_1^\top \Pi)^\dagger S_1 V_1^\top$$

By the definition of the condition number κ_+ , one needs to compute σ_{\min}^+ and σ_{\max}^+ where:

$$\sigma_{\min \setminus \max}^+ = \min \setminus \max_{\mathbf{x} \perp \ker((S_1 V_1^\top \Pi)^\dagger S_1 V_1^\top)} \frac{\|(S_1 V_1^\top \Pi)^\dagger S_1 V_1^\top \mathbf{x}\|}{\|\mathbf{x}\|}$$

Note that $\text{im } W_2 B_2^\top = \text{im } V_1 = \text{im } V_1 S_1$, so by [Theorem 4.12](#), $\ker \Pi \cap \text{im } V_1 S_1 = \{0\}$, hence $\ker \Pi V_1 S_1 = \ker V_1 S_1$. Since $\ker V_1 S_1 \cap \text{im } S_1 V_1^\top = \{0\}$, one gets $\ker \Pi V_1 S_1 \cap \text{im } S_1 V_1^\top = \{0\}$. By the properties of the pseudo-inverse $\ker \Pi V_1 S_1 = \ker (S_1 V_1^\top \Pi)^\top = \ker (S_1 V_1^\top \Pi)^\dagger$; as a result, $\ker ((S_1 V_1^\top \Pi)^\dagger S_1 V_1^\top) = \ker S_1 V_1^\top$. Since S_1 is invertible, $\ker ((S_1 V_1^\top \Pi)^\dagger S_1 V_1^\top) = \ker V_1^\top$.

For $\mathbf{x} \in \ker V_1^\top \Rightarrow \mathbf{x} \in \text{im } V_1$, so $\mathbf{x} = V_1 \mathbf{y}$. Since $V_1^\top V_1 = I$, $\|\mathbf{x}\| = \|V_1 \mathbf{y}\|$ and:

$$\sigma_{\min \setminus \max}^+ = \min \setminus \max_{\mathbf{y}} \frac{\|(S_1 V_1^\top \Pi)^\dagger S_1 \mathbf{y}\|}{\|\mathbf{y}\|} \stackrel{z=S_1 \mathbf{y}}{=} \min \setminus \max_z \frac{\|(S_1 V_1^\top \Pi)^\dagger \mathbf{z}\|}{\|S_1^{-1} \mathbf{z}\|}$$

Note that $\mathbf{v} = (S_1 V_1^\top \Pi)^\dagger \mathbf{z} \iff \begin{cases} S_1 V_1^\top \Pi \mathbf{v} = \mathbf{z} \\ \mathbf{v} \perp \ker S_1 V_1^\top \Pi \end{cases}$ and $\ker S_1 V_1^\top \Pi = \ker V_1^\top \Pi$, so:

$$\sigma_{\min \setminus \max}^+ = \min \setminus \max_{\mathbf{v} \perp \ker V_1^\top \Pi} \frac{\|\mathbf{v}\|}{\|V_1^\top \Pi \mathbf{v}\|}$$

Hence $\kappa_+ (C^\dagger P_\Sigma L_1^\dagger P_\Sigma^\top C^{\dagger\top}) = \kappa_+^2 (V_1^\top \Pi) = \kappa_+^2 (\Pi V_1)$.

□

Proposition 4.14. *The structure of the matrix ΠV_1 from [Theorem 4.13](#) provides a strategy for optimizing subsampling quality. Note that by the definition, the subsampling matrix Π is diagonal and binary, hence the best conditioning is achieved at $\Pi = I$ with $\kappa_+^2(V_1) = 1$, so one should minimize the distance between ΠV_1 and V_1 . Since $\text{span } V_1 = \text{im } W_2 B_2^\top = W_2 \text{im } B_2^\top$, V_1 is naturally scaled by the weight matrix W_2 , i.e. i -th row of V_1 is scaled by $w(t_i)$. Similarly, the subsampling matrix Π multiplies each row of V_1 either by 1 or 0; as a result, in order to close the distance between V_1 and ΠV_1 , one may aim to align 0s in the diagonal of Π with smallest weights in W_2 . In other words, one should search for heavier collapsible subcomplexes \mathcal{L} to achieve better preconditioning quality.*

4.5.1 Constructing Heavy Subcomplex out of 2-Core

Given [Theorem 4.13](#) and [Theorem 4.14](#), we search for a weakly collapsible subcomplex with a high total weight:

$$\max_{\mathcal{L} \in \Omega_{\mathcal{K}}} \|W\Pi(\mathcal{L})\|_F \quad \text{where} \quad \Omega_{\mathcal{K}} = \{\mathcal{L} \mid \mathcal{L} \subseteq \mathcal{K} \text{ and } \mathcal{L} \text{ is weakly collapsible}\}.$$

The [Algorithm 2](#) works as follows: start with an empty subcomplex \mathcal{L} ; then, at each step try to extend \mathcal{L} with the heaviest unconsidered triangle t : $\mathcal{L} \rightarrow \mathcal{L} \cup \{t\}$ ¹. If the extension $\mathcal{L} \cup \{t\}$ is weakly collapsible, it is accepted as the new \mathcal{L} , otherwise t is rejected; in either case triangle t is not considered for the second time.

Algorithm 2 HEAVY_SUBCOMPLEX(\mathcal{K}, W_2): construction a heavy collapsible sub-complex

Require: the original complex \mathcal{K} , weight matrix W_2

- 1: $\mathcal{L} \leftarrow \emptyset, \mathbb{T} \leftarrow \emptyset$ ▷ initial empty subcomplex
 - 2: **while** there is unprocessed triangle in $\mathcal{V}_2(\mathcal{K})$ **do**
 - 3: $t \leftarrow \text{nextHeaviestTriangle}(\mathcal{K}, W_2)$ ▷ e.g. iterate through $\mathcal{V}_2(\mathcal{K})$ sorted by weight
 - 4: **if** $\mathcal{L} \cup \{t\}$ is weakly collapsible **then** ▷ run GREEDY_COLLAPSE($\mathcal{L} \cup \{t\}$) ([Algorithm 1](#))
 - 5: $\mathcal{L} \leftarrow \mathcal{L} \cup \{t\}, \mathbb{T} \leftarrow [\mathbb{T} \ t]$ ▷ extend \mathcal{L} by t
 - 6: **end if**
 - 7: **end while**
 - 8: **return** $\mathcal{L}, \mathbb{T}, \Sigma$ ▷ here Σ is the collapsing sequence of \mathcal{L}
-

Remark 4.15 (Validity of [Algorithm 2](#)). The subcomplex \mathcal{L} sampled with [Algorithm 2](#) satisfies [Problem 1](#): indeed, $\mathcal{V}_0(\mathcal{K}) = \mathcal{V}_0(\mathcal{L})$, $\mathcal{V}_1(\mathcal{K}) = \mathcal{V}_1(\mathcal{L})$ and \mathcal{L} is weakly collapsible by construction. It is less trivial to show that the subsampling \mathcal{L} does not increase the dimensionality of 1-homology.

Assuming the opposite, the subcomplex \mathcal{L} cannot have any additional 1-dimensional holes in the form smallest-by-inclusion cycles of more than 3 edges: since this cycle is not present in \mathcal{K} , it is “covered” by at least one triangle t which necessarily has a free edge, so \mathcal{L} can be extended by t and remain weakly collapsible. Alternatively, if the only additional hole correspond to the triangle t not present in \mathcal{L} ; then, reminiscent of the proof for [Theorem 4.7](#), let us consider the minimal by inclusion simplicial complex \mathcal{K} for which it happens. Then the only free edges in \mathcal{L} are the edges of t , otherwise \mathcal{K} is not minimal. At the same time, in such setups t is not registered as a hole since it is an outer boundary of the complex \mathcal{L} , e.g. consider the exclusion of exactly one triangle in the tetrahedron case, [Figure 4.2](#)², which proves that \mathcal{L} cannot extend the 1-homology

¹here the extension implies the addition of the triangle t with all its vertices and edges to the complex \mathcal{L}

²algebraically, this fact is extremely dubious: due to the lack of free edges, there is a “path” between any two triangles in \mathcal{L} adjacent to t through adjacent triangles in \mathcal{L} , which reduces degrees of freedom in the circulation of the flow around t and brings it to $\ker B_2^\top$.

of \mathcal{K} .

The complexity of Algorithm 2 is $\mathcal{O}(m_1 m_2)$ at worst which could be considered comparatively slow: the algorithm passes through every triangle in $\mathcal{V}_2(\mathcal{K})$ and performs collapsibility check via Algorithm 1 on \mathcal{L} which never has more than m_1 triangles since it is weakly collapsible. Note that Algorithm 2 and Theorem 4.13 do not depend on \mathcal{K} being a 2-Core; moreover, the collapsible part of a generic \mathcal{K} is necessarily included in the subcomplex \mathcal{L} produced by Algorithm 2. Hence a prior pass of $\text{GREEDY_COLLAPSE}(\mathcal{K})$ reduces the complex to a smaller 2-Core \mathcal{K}' with faster $\text{HEAVY_SUBCOMPLEX}(\mathcal{K}', W_2)$ since $\mathcal{V}_1(\mathcal{K}') \subset \mathcal{V}_1(\mathcal{K})$ and $\mathcal{V}_2(\mathcal{K}') \subset \mathcal{V}_2(\mathcal{K})$.

We summarise the whole procedure in Figure 4.5: in order to construct the preconditioner C , one reduces a generic simplicial complex \mathcal{K} to a 2-Core \mathcal{K}' through the collapsing sequence Σ_1 and the corresponding sequence of maximal faces \mathbb{T}_1 ; then, a heavy weakly connected subcomplex \mathcal{L} is sampled from \mathcal{K}' with the collapsing sequence Σ_2 and the corresponding sequence of maximal faces \mathbb{T}_2 . The preconditioner C is formed by the subset of triangles $\mathbb{T}_1 \cup \mathbb{T}_2$ (that produces the projection matrix Π) with collapsing sequence (Σ_1, Σ_2) .

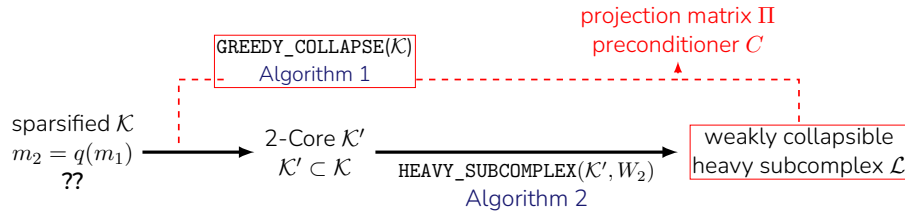


Figure 4.5: The scheme of the simplicial complex transformation: from the original \mathcal{K} to the heavy weakly collapsible subcomplex \mathcal{L} .

We refer to the preconditioner built according to Figure 4.5 via Algorithm 1 and Algorithm 2 as a *heavy collapsible subcomplex (HeCS)* preconditioner.

4.5.2 Cholesky decomposition for weakly collapsible subcomplex

4.5.3 Problem: precondition by subcomplex

4.5.4 Optimal weights for subsampling

4.5.5 Theorem on conditionality of a subcomplex

4.5.6 The notion of the heavy collapsible subcomplex

4.5.7 Algorithm and complexity

4.6 Benchmarking: triangulation

4.6.1 Timings of algorithm and preconditioned application

4.6.2 Conditionality and iterations

4.6.3 Compare with shifted chol

Chapter 5

Conclusion and future prospects

Bibliography

- [1] Lek-Heng Lim. Hodge Laplacians on Graphs. *SIAM Review*, 62(3):685–715, January 2020. ISSN 0036-1445. doi: 10.1137/18M1223101.
- [2] Phil Hanlon. The Laplacian Method. In Sergey Fomin, editor, *Symmetric Functions 2001: Surveys of Developments and Perspectives*, NATO Science Series, pages 65–91, Dordrecht, 2002. Springer Netherlands. ISBN 978-94-010-0524-1. doi: 10.1007/978-94-010-0524-1_2.
- [3] John Henry Constantine Whitehead. Simplicial spaces, nuclei and m-groups. *Proceedings of the London mathematical society*, 2(1):243–327, 1939.
- [4] Martin Tancer. Recognition of collapsible complexes is NP-complete. *Discrete & Computational Geometry*, 55:21–38, 2016.
- [5] Michael B. Cohen, Brittany Terese Fasy, Gary L. Miller, Amir Nayyeri, Richard Peng, and Noel Walkington. Solving 1-laplacians in nearly linear time: Collapsing and expanding a topological ball. In *Proceedings of the Twenty-Fifth Annual ACM-SIAM Symposium on Discrete Algorithms*, pages 204–216. SIAM, 2014.
- [6] Martin Tancer. D-collapsibility is NP-complete for $d \geq 4$. *Electronic Notes in Discrete Mathematics*, 34:53–57, 2009.
- [7] Davide Lofano and Andrew Newman. The worst way to collapse a simplex. *Israel Journal of Mathematics*, 244(2):625–647, 2021.
- [8] Michael T. Schaub, Austin R. Benson, Paul Horn, Gabor Lippner, and Ali Jadbabaie. Random Walks on Simplicial Complexes and the Normalized Hodge 1-Laplacian. *SIAM Review*, 62(2):353–391, January 2020. ISSN 0036-1445. doi: 10.1137/18M1201019.